88P

JPL PUBLICATION 86-36

CR

IN-28833

# Approximations Useful for the Prediction of Electrostatic Discharges for Simple Electrode Geometries

Larry Edmonds



August 15, 1986

National Aeronautics and Space Administration

Jet Propulsion Laboratory
California Institute of Technology
Pasadena, California

TECHNICAL REPORT STANDARD TITLE PAGE

| 1. Report No. JPL PUB 86-36 | 2. Government Accession No. | 3. Recipient's Catalog No. |
|---|---|---|

**4. Title and Subtitle**

Approximations Useful for the Prediction of Electrostatic Discharges for Simple Electrode Geometries

**5. Report Date**
August 15, 1986

**6. Performing Organization Code**

**7. Author(s)**
Larry Edmonds

**8. Performing Organization Report No.**

**9. Performing Organization Name and Address**

JET PROPULSION LABORATORY
California Institute of Technology
4800 Oak Grove Drive
Pasadena, California 91109

**10. Work Unit No.**

**11. Contract or Grant No.**
NAS7-918

**13. Type of Report and Period Covered**

JPL Publication

**12. Sponsoring Agency Name and Address**

NATIONAL AERONAUTICS AND SPACE ADMINISTRATION
Washington, D.C. 20546

**14. Sponsoring Agency Code**
RE230 BK-506-54-00-00-00

**15. Supplementary Notes**

**16. Abstract**

@ A35

This report provides approximations for estimating the capacitance and the ratio of electric field strength to potential for a certain class of electrode geometries. The geometry consists of an electrode near a grounded plane, with the electrode being a surface of revolution about the perpendicular to the plane. Some examples which show the accuracy of the capacitance estimate and the accuracy of the estimate of electric field over potential can be found in the appendix. When it is possible to estimate the potential of the electrode, knowing the ratio of electric field to potential will help to determine if an electrostatic discharge is likely to occur. Knowing the capacitance will help to determine the strength of the discharge (the energy released by it) if it does occur. A brief discussion of discharge mechanisms is given. The medium between the electrode and the grounded plane may be a neutral gas, a vacuum, or an uncharged homogeneous isotropic dielectric.

@ A35 Author

| 17. Key Words (Selected by Author(s)) | 18. Distribution Statement |
|---|---|
| Physics (General)<br>Electricity and Magnetism | Unclassified<br>Distribution Unlimited |

| 19. Security Classif. (of this report) | 20. Security Classif. (of this page) | 21. No. of Pages | 22. Price |
|---|---|---|---|
| Unclassified | Unclassified | | |

JPL PUBLICATION 86-36

# Approximations Useful for the Prediction of Electrostatic Discharges for Simple Electrode Geometries

Larry Edmonds

August 15, 1986

NASA
National Aeronautics and
Space Administration

**Jet Propulsion Laboratory**
California Institute of Technology
Pasadena, California

The research described in this publication was carried out by the Jet Propulsion Laboratory, California Institute of Technology, under a contract with the National Aeronautics and Space Administration.

## ABSTRACT

This report provides approximations for estimating the capacitance and the ratio of electric field strength to potential for a certain class of electrode geometries. The geometry consists of an electrode near a grounded plane, with the electrode being a surface of revolution about the perpendicular to the plane. Some examples which show the accuracy of the capacitance estimate and the accuracy of the estimate of electric field over potential can be found in the appendix. When it is possible to estimate the potential of the electrode, knowing the ratio of electric field to potential will help to determine if an electrostatic discharge is likely to occur. Knowing the capacitance will help to determine the strength of the discharge (the energy released by it) if it does occur. A brief discussion of discharge mechanisms is given. The medium between the electrode and the grounded plane may be a neutral gas, a vacuum, or an uncharged homogeneous isotropic dielectric.

CONTENTS

CONTENTS (continued)

## INTRODUCTION

Electrostatic discharges (ESD) are a potential hazard to spacecraft operations and many anomalies have been caused by them (Refs. 1 and 2). The job of the spacecraft designer will be made easier if a simplified method is developed to identify potential ESD-related hazards. If a situation is suspected of being an ESD-related hazard, a detailed analysis is required, except under conditions where a simplified analysis can confidently show that the suspected hazard is really not a hazard. Since a detailed analysis is expensive, it is desirable to narrow the list of suspected hazards as much as possible using simplified methods.

This report provides approximations that can help determine, for a certain class of electrode geometries, if an electrostatic discharge will occur, and determine an upper bound on the strength of the discharge (the energy released by it) if it does occur. The approximations that are provided are estimates of the electric field strength, as a function of electrode potential and geometry, and estimates of capacitance.

When using analytical methods to solve for quantities such as electric field or capacitance, it is typical to simplify the problem by assuming the geometry to have some kind of symmetry. The two kinds of symmetries that have enough generality to provide acceptable approximations for a large number of real situations are (1) translational symmetry in a specified direction, and (2) rotational symmetry about some axis. An important example of the first kind of symmetry is a long, straight wire parallel to a plane. It is relatively easy to obtain approximate solutions for electrostatic problems having translational symmetry. A lot of simple geometries have already been solved analytically. For example, the solution for a single wire or even a grid of wires parallel to a plane has been solved and the solutions can be found in Ref. 3. If the geometry does not have a known analytic solution and if the well-known analytic methods (e.g., conformal transformations) are difficult to apply, there is a graphical method for obtaining quick estimates for quantities like capacitance and electric field strength. This graphical method is described in Ref. 4. The rotational symmetry is more difficult. Unless the geometry is one of the few that can be solved analytically, the only general methods for solving these problems are numerical methods that require a computer. Most engineers do not have the computer codes and, therefore, there is a need for simplified methods to obtain approximate solutions. That is the subject of this report. The geometries that will be treated in this report consist of an electrode, which is a surface of revolution, near a grounded plane. The axis of symmetry of the electrode is perpendicular to the plane.

Most electrostatic characteristics of an electrode and grounded plane are equivalent to those of two electrodes of equal but opposite potentials, with one electrode the mirror image of the other. Therefore, the results given in this report can also be applied to that arrangement. There is a subtle difference between the two arrangements in terms of energy released by the discharge, as discussed in Section 3. The upper bound on the strength of the discharge, as estimated in Section 3, will require that the electrode be everywhere convex. However, this is not a serious limitation. If the actual electrode surface is not everywhere convex, it can be replaced by an imaginary surface that completely surrounds the actual surface and that is everywhere

convex. Applying the analysis to this imaginary electrode will produce an upper bound on the energy released by it and on the energy released by the actual electrode as well.

The material in this report is applicable when the medium between the electrodes is either neutral gas, a vacuum, or an uncharged homogeneous isotropic dielectric. The admittedly important case of a plasma between the electrodes is not treated here. If a plasma is present, a space charge will be set up, and the potential will not satisfy Laplace's equation. The field patterns described in this report do not apply. Furthermore, there are indications that a discharge is controlled by the local field induced by an ion and its image charge, rather than by the macroscopic or average field (Ref. 5). Therefore, it is not clear whether knowledge of the macroscopic field would even be useful. The subject of a plasma is specialized and requires a treatment that is beyond the scope of this report.

In an effort to make this report easy for engineers to use, discussions related to applications have been separated from the theoretical derivations of the equations. Part I of this report is applications oriented and does not contain the theoretical justifications of the equations. It is self-contained in the sense that it explains how the equations are to be used, without requiring that the reader understand where the equations came from. Part II gives the theoretical derivations of all of the equations given in Part I.

To predict the occurrence of an electrostatic discharge, depending on the discharge mechanism, it is sometimes enough to know the strength of the electric field at the apex of the electrode (it is assumed that the field is most intense there). This is the subject of Section 1. Under other circumstances, the electric field must be known at other locations. This is discussed in Section 2. Energy and capacitance are treated in Section 3. Section 4 provides information on what to do about surface deformities, flaws in the shape of the surface, which cause it to differ from an ideal smooth shape. The main emphasis is placed on the surface microstructure. At first glance, an electrode surface may appear to be smooth with a well-defined radius of curvature, but a closer look under magnification shows tiny scratches, dents and protrusions. The question arises as to which radius of curvature (the radius of curvature seen without the magnification or the radius of curvature of the microscopic protrusions) should be used in the equations presented in this report, i.e., should an estimate of the electric field in "the large" be made or should the local electric field near the protrusions be estimated. This is immaterial to the capacitance estimate but it is an important question when predicting the occurrence of an electrostatic discharge. The answer to this question depends on which kind of discharge mechanism will be in control if a discharge does occur. Section 4, which attempts to answer this question, combines a discussion of surface deformities with a brief discussion of some basic concepts related to discharge mechanisms. The physical processes that control the occurrence of an electrostatic discharge are complex, and a thorough discussion is beyond the scope of this report. Section 4 is not intended to be an exhaustive review, and it is not self-contained in the sense of providing the empirical data necessary to predict the occurrence of a breakdown. The reader will have to investigate other references to find that information. The discussion of discharge mechanisms is only intended to give an idea as to what level of magnification must be looked at in order to predict a breakdown.

The appendix contains a list of example electrode geometries. Each geometry listed is accompanied by the error obtained by using the equations given in this report. If the reader is fortunate, he may find that his electrode is almost exactly represented in one of the examples. It is more probable that he will find it to lie somewhere between two geometries used in the examples. The error given for the two examples will give the reader an idea as to what kind of errors he can expect when he applies these equations to his geometry.

# PART I - APPLICATIONS

# SECTION 1

## ELECTRIC FIELD AT APEX

It is possible to estimate the potential of various parts of a spacecraft using the methods found in Refs. 1 and 6. This estimate must be done before any assessment can be made of ESD-related hazards. Therefore, it will be assumed that this has already been done. The potential of the electrode is then taken as a known quantity. This information is not enough to predict the occurrence of an electrostatic discharge, because it is the electric field strength, rather than the potential, that is the controlling influence. The information that is missing is a relationship between electric field and potential, and this relationship depends on the geometry of the electrode. Under some circumstances, to predict a breakdown (at least in a probabilistic sense), it is enough to know the electric field strength at the location where the electric field is most intense. That is the subject of this section. It is assumed that the electrode is convex near the end closest to the plane (although in this section it need not be everywhere convex), so the maximum electric field is at the apex of the electrode.

Let the apex have a radius of curvature R and be a distance L from the grounded plane, and let V and E be the potential and electric field, respectively, at the apex. An approximate relationship between V and E is

$$\frac{V}{E} = \frac{LR}{\frac{2L + R}{3}} . \tag{1.1}$$

We can qualitatively see why Eq. (1.1) might be expected to be a good approximation in the following way. Define K to satisfy

$$\frac{V}{E} = \frac{LR}{KL + R} \tag{1.2}$$

which can be solved for K giving

$$K = \frac{(LE - V)}{V} \frac{R}{L} . \tag{1.3}$$

If we change one variable on the right side of Eq. (1.3) by changing the geometry, another variable tends to make a compensating change, allowing K to change by only a small amount. For example, if we increase R without changing L, the electric field will become more uniform and the term (LE-V)/V, which is the fractional error obtained by approximating the potential with the potential from a uniform field, gets smaller. So K has one tendency to increase due to the R on the right side of Eq. (1.3), and another tendency to decrease due to the decrease in (LE-V)/V. The two tendencies compete with one another and partially compensate for each other. The result is that K is not very sensitive to the geometry. This is equivalent to saying that most of the variation (with geometry) of V/E is accounted for by the L and R on the right side of Eq. (1.2). Only small changes (with geometry) in K are needed to balance the remaining variation in V/E. This indicates that if Eq. (1.2) is applied to an equipotential surface created by the electrode (so that V, E, L,

R, and K now refer to the equipotential surface instead of the electrode), the value of K will be nearly the same for each equipotential surface. In other words, K is a slowly varying function of the equipotential surface with which it is associated. This means that its value, for any equipotential surface, and in particular for the electrode surface, can be approximated by the limiting value as we look at surfaces closer and closer to the plane. It is shown in Part II that this limiting value is 2/3. This result follows from very general considerations, requiring only that the potential possess the assumed symmetry, and that it satisfy Laplace's equation. Replacing K with 2/3 produces Eq. (1.1).

The above discussion explains why Eq. (1.1) provides an approximation for V/E, but it doesn't quantitatively answer the question of how good the approximation is. This is best seen by referring to the examples in the appendix. In these examples the approximation is usually accurate to within 20 percent.

Although Eq. (1.1) is usually accurate, the accuracy does depend on the geometry, and the reader may have a geometry that isn't well represented by any of the examples in the appendix. Therefore, the error may be difficult to anticipate. It would be nice to have upper and lower bounds on V/E for situations like this. For a certain class of geometries, described below, there is a simple upper and lower bound. Assume that the geometry is of such a nature that the equipotential surfaces are all convex in the immediate neighborhood of the axis of symmetry. Assume also that the electrode is sufficiently pointed and elongated in the direction of the axis of symmetry so that the electric field lines near the axis of symmetry bend towards the axis as we move from the electrode to the plane. This is illustrated in Fig. 1.1. It is shown in Part II that when these conditions are satisfied, V/E is bounded by:

$$\frac{LR}{L+R} \leq \frac{V}{E} \leq L \quad . \tag{1.4}$$

Determining if the geometric conditions required for the validity of Inequality (1.4) are satisfied requires some ability to visualize the electric field pattern. For some geometries this is not easy to do. Fortunately, for many geometries (e.g., cigar-shaped electrodes), it is easy to see that the field pattern will have the required properties, and Inequality (1.4) can be used with confidence.

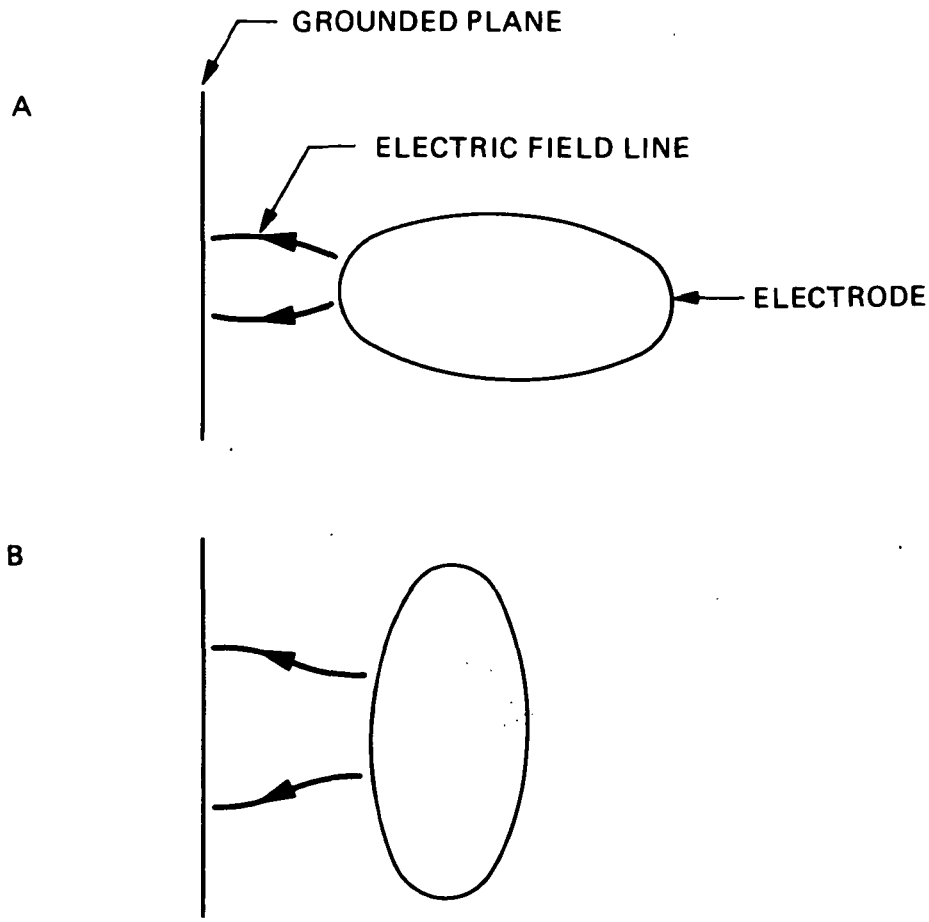


Fig. 1.1 Two examples of electric field patterns.

In Figure A, the equipotential surfaces are convex (the electric field lines are spreading apart) and the electric field lines bend towards the axis as we move towards the plane. In Figure B, the equipotential surfaces are convex but the electric field lines bend away from the axis at some locations.

## SECTION 2

## FIELD PATTERN BETWEEN ELECTRODE AND PLANE

Depending on the user's needs, it may be useful to know not only the electric field at the apex but also the way the field varies in space. Depending on the discharge mechanism, the prediction of a discharge could require this information. That is the subject of this section.

The field pattern described in this section will be called the "model field." The model field is defined to be the special field that satisfies Eq. (1.1) exactly, not only at the electrode, but also at every equipotential surface created by the electrode. Equation (1.1) is typically a good approximation for each equipotential surface, so the model field serves as an approximation for the actual field.

Throughout this report, the coordinate system is oriented so that the axis of symmetry is the Z axis, and the grounded plane is at Z = 0 and is the XY plane. The apex of the electrode is on the Z axis at Z = L. The potential at a point in space is denoted by $\phi$, and V is the potential of the electrode, so that $\phi = V$ when evaluated on the electrode surface.

### A. FIELD ON AXIS

It is shown in Part II that on the axis of symmetry, the potential, as a function of Z, for the model field is given by

$$\phi(Z) = \frac{V}{L} Z \frac{\left[1 - \left(\frac{L}{M}\right)^2\right]^{1/2}}{\left[1 - \left(\frac{Z}{M}\right)^2\right]^{1/2}} \tag{2.1}$$

where M is defined by

$$M^2 = L^2 + \frac{3}{2} LR \quad . \tag{2.2}$$

The magnitude of the electric field is given by

$$E(Z) = \frac{V}{L} M^2 \frac{[M^2 - L^2]^{1/2}}{[M^2 - Z^2]^{3/2}} \quad . \tag{2.3}$$

The right side of Eq. (2.1) is the potential, VZ/L, that would result from a uniform electric field times a modulating factor $[1 - (L/M)^2]^{1/2}/[1 - (Z/M)^2]^{1/2}$. At points sufficiently close to the plane, the modulating factor is nearly constant and the potential is nearly linear in Z. Furthermore, if R>>L, the modulating factor will be nearly equal to 1 everywhere between the plane and electrode so the potential resembles the potential from a uniform electric field everywhere between the plane and electrode. For other combinations of Z, L, and R, the modulating factor can have an important effect on the variation of $\phi$.

## B. FIELD OFF AXIS-SERIES SOLUTION

Let r be the distance from the origin to a point in space and $\theta$ be the angle between the position vector (measured from the origin) of the point and the Z axis. It is shown in Part II that the potential, expressed as a function of r and $\theta$, can be written as

$$\phi(r,\theta) = RE_L \sum_{n=o}^{\infty} A_n(r)\rho_{2n+1}(\cos\theta) \qquad r < M \tag{2.4}$$

where

$$E_L = \frac{(M^2 - L^2)^{1/2}}{M} \frac{V}{L}$$

with M given by Eq. (2.2). $\rho_n(\cos\theta)$ are the Legendre polynomials and $A_n$ is given by

$$A_o(r) = r/R$$

$$A_n(r) = \frac{(2n-1)!\,(r/R)^{2n+1}}{n!(n-1)!2^{2n-1}\,(M/R)^{2n}} \qquad n \geq 1 .$$

For the purpose of numerical evaluation of Eq. (2.4), it is most convenient to evaluate the Legendre polynomials by using

$$\rho_o(x) = 1 \qquad \rho_1(x) = x$$

and the recursion formula (see page 541, Ref. 17)

$$\rho_{n+1}(x) = 2x\rho_n(x) - \rho_{n-1}(x) - [x\rho_n(x) - \rho_{n-1}(x)]/(n+1) .$$

$A_n$ is most conveniently evaluated by starting with $A_o(r) = r/R$ and using the recursion formula

$$A_{n+1}(r) = \frac{(2n+1)\left(\frac{r}{R}\right)^2}{2(n+1)\left(\frac{M}{R}\right)^2} A_n(r) \qquad n \geq o .$$

The reader should be aware that the series in Eq. (2.4) has a finite radius of convergence. It converges only for $r < M$. As r approaches M the convergence becomes very slow, and large numbers of terms are needed for a numerical evaluation.

## C. FIELD OFF AXIS-INTEGRAL SOLUTION

Unless r is much smaller than M, the series in Eq. (2.4) converges very slowly, and large numbers of terms are needed for a numerical evaluation. For numerical evaluation, Eq. (2.4) has little advantage over an integral representation of the solution. An integral representation has the advantage that analytic properties of a function are typically more visible than in a series representation.

If the potential is evaluated in the XZ plane, a point of evaluation can be assigned just the two coordinates X and Z. It is shown in Part II that the potential (for $X^2 + Z^2 < M^2$) can be expressed as

$$\phi(X,Z) = \frac{V}{\pi L}(M^2 - L^2)^{1/2} \, ZRe \int_0^{\pi} \frac{r^2 + iMX\cos\theta \, d\theta}{[r^2 - X^2\cos^2\theta\,]\sqrt{M^2 - r^2 - 2iMX\cos\theta}} \qquad (2.5)$$

where $r = [X^2 + Y^2]^{1/2}$, i is the imaginary number and Re denotes "real part of." The square root in Eq. (2.5) is the principal determination of the square root of a complex number. As with the series solution (Eq. 2.4), the integral solution (Eq. 2.5) is valid only for $r < M$. Steps for obtaining a solution valid for $r > M$ are suggested in Part II, although it is probably not worth the effort, because the model field will not be a good approximation of the actual field (except for a special electrode geometry) if we get too far away from the axis of symmetry.

A Fortran subroutine that evaluates the potential using Eq. (2.5) is given in Fig. 2.1. The variables sent to the subroutine are the X and Z coordinates of the point of evaluation of the potential. These coordinates have been made dimensionless by dividing by M (Eq. 2.2), i.e., they are distances measured in units of M. The "potential" returned by the subroutine is also dimensionless and is actually $\pi L/V\sqrt{M^2 - L^2}$ times the potential $\phi$ given by Eq. (2.5). $\phi$ is obtained by multiplying the value returned by the subroutine by $V\sqrt{M^2 - L^2}/\pi L$.

```
      SUBROUTINE VOLT1(X,Z,V)
C  USED WHEN R<=1
      DOUBLE PRECISION X,Z,V,DTHETA,R,R1,R2,R3,THETA,
     +THETA1,THETA2,PI,CS,SUM,A
      R=DSQRT(X*X+Z*Z)
      PI=2D0*DATAN2(1D0,0D0)
      SUM=0D0
      DTHETA=PI/2D3
      THETA=-DTHETA/2D0
      DO 10 J=1,2000
      THETA=THETA+DTHETA
      CS=DCOS(THETA)
      R3=X*X*CS*CS-R*R
      R1=DSQRT(R*R*R*R+X*X*CS*CS)
      R2=DSQRT((1D0-R*R)*(1D0-R*R)+4D0*X*X*CS*CS)
      THETA1=DATAN2(X*CS,R*R)
      THETA2=DATAN2(-2D0*X*CS,1D0-R*R)
      A=DCOS(THETA1-THETA2/2D0)
      A=A*R1/R3
      A=A/DSQRT(R2)
      SUM=A+SUM
 10   CONTINUE
      V=-Z*DTHETA*SUM
      RETURN
      END
```

Fig. 2.1 Fortran subroutine using Eq. (2.5).

## SECTION 3

## ENERGY AND CAPACITANCE

Once it has been determined that an electrostatic discharge could occur, the next question is how much of a disturbance can it make, i.e., how much energy can it force into a system such as a nearby electronic circuit. An upper bound on this energy is all of the energy stored in the electrostatic field which is related to the capacitance of the electrode. An upper bound on the energy stored in the field and the capacitance of the electrode is the subject of this section.

If an electrode is placed in front of a grounded plane, the field pattern on the electrode side of the plane is identical to what would be obtained if the plane were removed and replaced with the familiar "image" electrode. In this respect, the two arrangements are indistinguishable. But in terms of capacitance or energy stored in the field, there is a distinction between the two arrangements. The grounded plane arrangement has only half as much energy stored in the field as the two electrode arrangement since the field lies in only one hemisphere of space. It sounds paradoxical that the two electrode case has twice as much energy available that can potentially be coupled into an electronic circuit (if the energy were converted to radiation) than the grounded plane case, even though the fields for the two cases are indistinguishable. The reconciliation is that the fields are only indistinguishable when nothing else is present. If a receiving antenna is introduced, the field patterns become distinguishable. If the grounded plane is replaced with the equivalent images, there will be an image antenna absorbing the "image half of the energy" so the real antenna can only interact with half as much energy as it could in the two electrode case. The capacitance is also different for the two arrangements. Capacitance between two objects is defined as charge over the potential difference between them, with the stipulation that they have equal but opposite charges. If Q is the charge on the electrode, the capacitance between the electrode and grounded plane is

$$C \text{ (grounded plane)} = \frac{Q}{V}$$

while the capacitance between the electrode and a similiar electrode (the image electrode, which is at potential $-V$ so that $2V$ is the potential difference between electrodes) is

$$C \text{ (two electrodes)} = \frac{Q}{2V} = \frac{1}{2}C \text{ (grounded plane)} \quad .$$

The energy stored in the field is one-half the capacitance times the square of the potential difference so

$$E \text{ (grounded plane)} = \frac{1}{2}C \text{ (grounded plane)} \, V^2 \qquad (3.1)$$

and

$$E \text{ (two electrodes)} = \frac{1}{2}C \text{ (two electrodes)}(2V)^2 = C \text{ (grounded plane) } V^2$$

$$= 2E \text{ (grounded plane)} .$$

When using capacitance to calculate energy stored in the field, the capacitance calculated for the correct physical system should be used or there will be an error of a factor of 2.

Although capacitance and energy depend on which arrangement we are looking at, it is trivial to convert these quantities from the grounded plane arrangement to the two electrode arrangement, and vice-versa, making it arbitrary as to which case is studied. For consistency, we will select a convention. Throughout the remainder of this report, the physical system under study will be the grounded plane arrangement. Also, the plane and electrode will be taken to be in empty space. If a homogeneous isotropic dielectric is present, the energy and capacitance can be calculated by first calculating them for free space and then multiplying by the relative dielectric constant.

Energy is related to capacitance by Eq. (3.1). It is shown in Part II that an approximation for the capacitance for an electrode that is everywhere convex is given by

$$C = \frac{8\pi\varepsilon_o}{BD} \frac{1}{\ln^2\left(\frac{1 + BL}{1 - BL}\right)} \int \frac{X}{\sqrt{(\vec{r}_L \cdot \hat{n})(\vec{r}_R \cdot \hat{n})}} \text{Tan}^{-1}\left(LB\sqrt{\frac{\vec{r}_R \cdot \hat{n}}{\vec{r}_L \cdot \hat{n}}}\right) d\ell \qquad (3.2)$$

where

$\varepsilon_o$ = permittivity constant = $8.85 \times 10^{-12}$ farads/meter

D = length of the electrode (i.e., distance between intercepts with the axis of symmetry)

L = distance between electrode and grounded plane

B = $1/\sqrt{L^2 + LD}$

$\vec{r}_L$ = position vector measured from the apex of the electrode that is closest to the grounded plane

$\vec{r}_R$ = position vector measured from the apex of the electrode that is furthest from the plane

$\hat{n}$ = unit vector normal to electrode surface

The integral in Eq. (3.2) is a line integral. The curve of integration is the +X half of the intersection of the electrode with the XZ plane. The X in Eq. (3.2) is the X coordinate of a point on the curve and $d\ell$ is an element of arc length. The quantities $\vec{r}_L$, $\vec{r}_R$, and $\hat{n}$ are evaluated at the appropriate point on the curve. The approximation given by Eq. (3.2) will always be an overestimate of the correct capacitance.

Although Eq. (3.2) has a formidable appearance, it is not difficult to evaluate numerically. An algorithm for doing this is: first obtain a graph of the shape of the electrode (the intersection of the electrode with the +X half of the XZ plane) and get the X and Z coordinates of N points that lie on this curve. The first of these N points should be close to (but not at) the apex of the electrode nearest the plane, and the last should be close to (but not at) the apex furthest from the plane. Then the integral in Eq. (3.2) can be approximated with the sum

$$\text{Integral} = \sum_{i=1}^{N-1} \frac{X_a(i)}{\sqrt{A_1(i)A_2(i)}} \text{Tan}^{-1}\left(LB\sqrt{\frac{A_2(i)}{A_1(i)}}\right)\Delta_i\ell \qquad (3.3)$$

where

$$\begin{aligned}
X(i),Z(i) &= \text{X and Z coordinates of the ith point}\\
X_a(i) &= 1/2\ (X(i) + X(i+1))\\
Z_a(i) &= 1/2\ (Z(i) + Z(i+1))\\
\Delta_i X &= X(i+1) - X(i)\\
\Delta_i Z &= Z(i+1) - Z(i)\\
\Delta_i \ell &= \sqrt{(\Delta_i X)^2 + (\Delta_i Z)^2}\\
A_1(i) &= (X_a(i)\Delta_i Z - (Z_a(i) - L)\Delta_i X)/\Delta_i \ell\\
A_2(i) &= (X_a(i)\Delta_i Z + (L+D - Z_a(i))\Delta_i X)/\Delta_i \ell
\end{aligned}$$

For a numerical example in using this algorithm, consider the electrode shown in Fig. 3.1. Capacitance depends on the overall size of the geometry, so we have to know how much distance each grid line of the graph represents. Suppose a major division represents one meter (a large electrode). The left apex is about 0.43 meters from the grounded plane, and the right is about 5.2 meters. Thus, L = 0.43 meters and the length of the electrode is about D = 5.2 - 0.43 = 4.77 meters. The coordinates (units are meters) of a number of points representing the curve are shown in the columns labelled Z(i) and X(i) in Table 3.1. Note that the first entry is not the coordinates of the left apex, but the coordinates of the representative point next to the apex. Similarly, the last entry does not refer to the right apex, but to the representative point next to it. A division by zero will result if this procedure is not followed. The terms in the sum in Eq. (3.3) are shown calculated in Table 3.1. The value of B used in the calculations is $B = 1/\sqrt{L^2 + LD} = 0.6688$ meters$^{-1}$. The individual terms are then added together to form the sum in Eq. (3.3). The units are meters. This sum approximates the integral in Eq. (3.2). It must then be multiplied by

$$\frac{8\pi\varepsilon_o}{BD}\,\frac{1}{\ln^2\left(\frac{1+BL}{1-BL}\right)} = \frac{8\pi(8.85\times10^{-12}\ \text{farads/meter})}{(0.6688)(4.77)}\,\frac{1}{\ln^2\left(\frac{1+(0.6688)(0.43)}{1-(0.6688)(0.43)}\right)}$$

$$= 1.990\times10^{-10}\ \frac{\text{farads}}{\text{meter}}\ .$$

The estimate of the capacitance is

$$C = \left(1.990\times10^{-10}\ \frac{\text{farads}}{\text{meter}}\right)\times(2.142\ \text{meters}) = 4.26\times10^{-10}\ \text{farads}\ .$$

The actual capacitance for this electrode happens to be known (through other methods); it is $3.56\times10^{-10}$ farads. In this example, the hand calculation was accurate to within 20 percent of the correct value.

While Eq. (3.2) represents a quantity that is larger than the actual capacitance, a numerical evaluation of the equation could underestimate the capacitance if the evaluation does not accurately represent the equation. The integration that is simulated by the numerical algorithm does not include the integral on the section of the curve that is between the apex and the first point (X(1), Z(1)). This is intentional, to avoid dividing by zero. The first point should be made close enough to the apex that this section of the curve represents an insignificant contribution to the capacitance. Also, the coordinates must be entered with enough precision to display the required convex nature of the curve. If the curve looks very flat, a lot of digits may have to be entered. Unless the points display some curvature near the apex, a division by zero will result.

It has been assumed that the curve is everywhere convex. This requirement is slightly stronger than is really necessary. Being everywhere convex is a sufficient condition for the calculational method to work, but the method will sometimes work (as can be seen in a few of the examples in the appendix) even if the curve is not everywhere convex. However, applying this calculational method to such a curve is likely to produce mathematically undefined quantities. Furthermore, the examples in the appendix show the largest errors for such curves. If the actual electrode does not have this convex property, it is suggested that it be replaced with a slightly larger ficticious electrode that encloses the actual electrode and that does have the required property. This may be necessary to avoid mathematically undefined terms. Even if it is not necessary, it is likely to produce greater accuracy. Applying Eq. (3.2) to the ficticious surface is likely to produce a smaller capacitance estimate than would be obtained by applying the equation to the actual electrode. Since both estimates are upper bounds on the correct capacitance, the smaller estimate is more accurate.

The capacitance estimates shown in the appendix are accurate to within 50 percent in the examples that are everywhere convex. A few examples show surfaces that are not everywhere convex but the capacitance estimate could still be made. In these examples the error is much larger. The examples also demonstrate the previously stated fact that the predicted capacitance is always greater than the correct capacitance. If a geometry is not well represented by any of the examples, the accuracy of Eq. (3.2) will be somewhat uncertain but it is certain that the estimate will be higher than the correct value.

The estimates produced by Eq. (3.2) are not highly accurate, the equation is intended for rough estimates. The purpose of these estimates is to serve as a preliminary study of potential ESD hazards to help determine if a more elaborate analysis is warranted. This is done by estimating upper bounds on the undesirable effects of an ESD, such as the energy coupled into a nearby circuit. There are a number of uncertainties in the problem, such as uncertainties in the voltage at which a discharge will occur, uncertainties in the spectrum of the ESD-induced electromagnetic radiation, and uncertainties in the coupling between the electromagnetic radiation and a nearby circuit. Given all of these uncertainties, an error in the capacitance estimate of even a factor of two (electrical engineers should read this as 3dB) is not bad for a preliminary investigation.

A Fortran code, which uses the same algorithm as the hand calculation of the previous example, is given in Fig. 3.2. The code assumes that an input data file exists. The first three entries of the data file are, respectively, L, D, and the number of interior points that will represent the curve. "Interior," in this case, means points between, but not at, the intercepts of the curve with the Z axis. The remaining entries of the data file are the Z and X coordinates of the interior points. Following the listing of the Fortran code is a sample input data file. This data file was constructed for the same electrode that was used in the hand calculation so the reader can compare the data file with Table 3.1 if there is any confusion. The units that are to be used are meters.

If the reader must routinely solve such problems so that a more elaborate computer code is justified, he should be aware that more accurate methods exist (e.g., a charge simulation technique where N point charges of unknown charge are placed on the Z axis inside the electrode and image charges are placed inside the image electrode. Specifying N points on the electrode surface produces N linear equations that are used to solve for the unknown charges). The advantage of the method given here is that it can be done by hand or quickly typed into a computer.

As an incidental remark, Eq. (3.2) is not the only upper bound on the capacitance. A systematic procedure for constructing upper bounds is described in Part II. This author has tried several, Eq. (3.2) being the best compromise between accuracy and simplicity, of the few that were tried. With trial and error, a better method may be found.

Table 3.1 Example hand calculation to estimate capacitance.

L = 0.43 B = 0.6688 D = 4.77

| i | Z(i) | X(i) | Za(i) | Xa(i) | ΔiZ | ΔiX | Δiℓ | $A_1(i)$ | $A_2(i)$ |
|---|---|---|---|---|---|---|---|---|---|
| 1 | .5 | .3 | .55 | .4 | .1 | .2 | .2236 | 7.156(-2) | 4.338 |
| 2 | .6 | .5 | .8 | .75 | .4 | .5 | .6403 | 1.796(-1) | 3.904 |
| 3 | 1.0 | 1.0 | 1.25 | 1.2 | .5 | .4 | .6403 | 4.248(-1) | 3.405 |
| 4 | 1.5 | 1.4 | 1.75 | 1.5 | .5 | .2 | .5385 | 9.025(-1) | 2.674 |
| 5 | 2.0 | 1.6 | 2.25 | 1.66 | .5 | .12 | .5142 | 1.189 | 2.303 |
| 6 | 2.5 | 1.72 | 2.75 | 1.75 | .5 | .06 | .5036 | 1.461 | 2.029 |
| 7 | 3.0 | 1.78 | 3.25 | 1.75 | .5 | -.06 | .5036 | 2.073 | 1.505 |
| 8 | 3.5 | 1.72 | 3.75 | 1.645 | .5 | -.15 | .522 | 2.530 | 1.159 |
| 9 | 4.0 | 1.57 | 4.25 | 1.435 | .5 | -.27 | .5682 | 3.078 | 8.113(-1) |
| 10 | 4.5 | 1.3 | 4.75 | 1.5 | .5 | -.6 | .781 | 4.279 | 6.146(-1) |
| 11 | 5.0 | .7 | 5.05 | .575 | .1 | -.25 | .2693 | 4.502 | 7.427(-2) |
| 12 | 5.1 | .45 | 5.125 | .35 | .05 | -.2 | .2062 | 4.639 | 1.212(-2) |
| 13 | 5.15 | .25 | ___ | ___ | ___ | ___ | ___ | ___ | ___ |

| i | $\frac{X_a(i)}{\sqrt{A_1(i)A_2(i)}}$ | $\mathrm{Tan}^{-1}\left(LB\sqrt{\frac{A_2(i)}{A_1(i)}}\right)\Delta_i\ell$ |
|---|---|---|
| 1 | 7.179(-1) x 2.573(-1) | = .1847 |
| 2 | 8.957(-1) x 5.955(-1) | = .5334 |
| 3 | 9.978(-1) x 4.376(-1) | = .4366 |
| 4 | 9.656(-1) x 2.475(-1) | = .2390 |
| 5 | 1.003 x 1.958(-1) | = .1964 |
| 6 | 1.016 x 1.646(-1) | = .1672 |
| 7 | 9.908(-1) x 1.210(-1) | = .1199 |
| 8 | 9.606(-1) x 1.004(-1) | = .0964 |
| 9 | 9.081(-1) x 8.330(-2) | = 7.564(-2) |
| 10 | 9.250(-1) x 8.479(-2) | = 7.843(-2) |
| 11 | 9.944(-1) x 9.943(-3) | = 9.888(-3) |
| 12 | 1.476 x 3.031(-3) | = 4.474(-3) |

Total = 2.142 meters

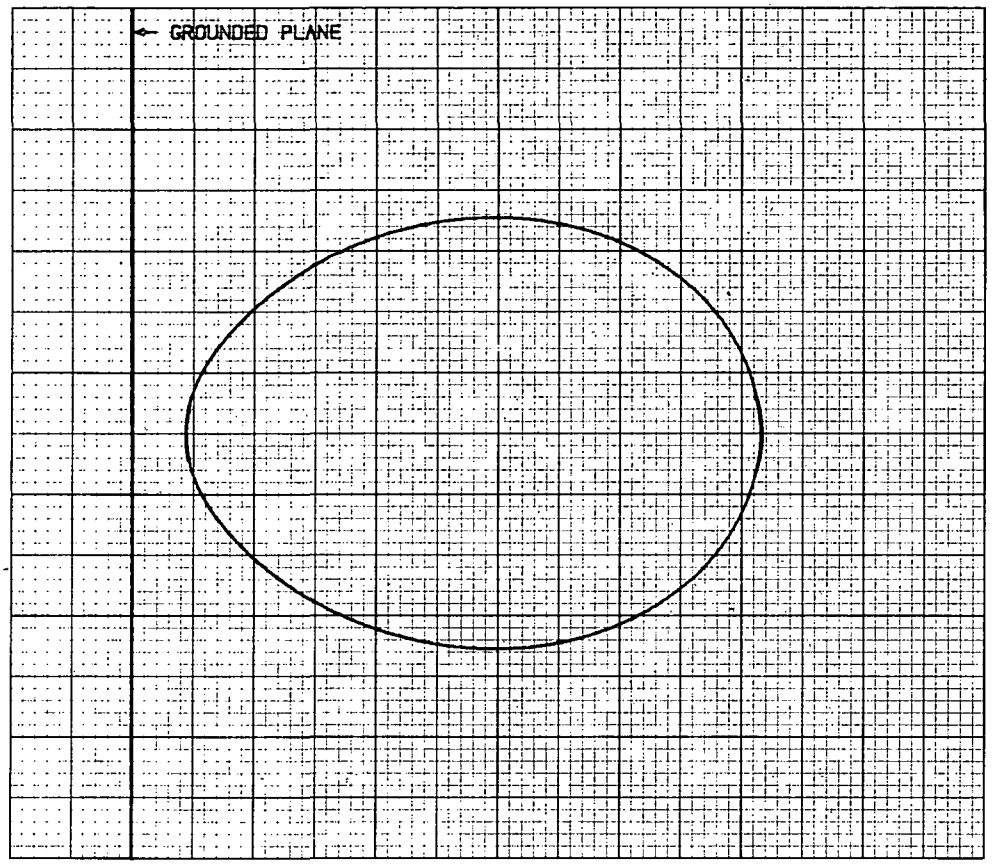


Fig. 3.1 Electrode used in the numerical example of the evaluation of Eq. (3.2).

```
      PROGRAM CAP
      DIMENSION Y(100),Z(100)
      REAL L,M
      OPEN(UNIT=9,FILE="CDATA",STATUS='OLD')
      REWIND(9)
      READ(9,*) L
      READ(9,*) D
      READ(9,*) N
      DO 10 I=1,N
      READ(9,*) Z(I),Y(I)
 10   CONTINUE
      M=SQRT(L*L+L*D)
      M=1.0/M
      S=0.0
      DO 20 I=1,N-1
      YI=(Y(I)+Y(I+1))/2.0
      ZI=(Z(I)+Z(I+1))/2.0
      DELTAZ=Z(I+1)-Z(I)
      DELTAY=Y(I+1)-Y(I)
      DELTAL=SQRT(DELTAZ*DELTAZ+DELTAY*DELTAY)
      A1=(YI*DELTAZ-(ZI-L)*DELTAY)/DELTAL
      A2=(YI*DELTAZ+(L+D-ZI)*DELTAY)/DELTAL
      W1=L*M*SQRT(A2/A1)
      W2=YI/(SQRT(A1*A2))
      SP=W2*ATAN(W1)*DELTAL
      S=S+SP
 20   CONTINUE
      Q=(1.0+M*L)/(1.0-M*L)
      Q=ALOG(Q)
      Q=1.0/(Q*Q)
      Q=(2.22E-10)*Q/(M*D)
      S=Q*S
      PRINT*,"CAPACITANCE = ",S," FARADS"
      END
```

SAMPLE INPUT DATA FILE NAMED CDATA

```
.43
4.77
13
.5,.3
.6,.5
1.0,1.0
1.5,1.4
2.0,1.6
2.5,1.72
3.0,1.78
3.5,1.72
4.0,1.57
4.5,1.3
5.0,.7
5.1,.45
5.15,.25
```

Figure 3.2 Fortran code for estimating capacitance.

## SECTION 4

## SURFACE DEFORMITIES AND DISCHARGE MECHANISMS

Surface deformities can be put into two categories, deformities in the large (i.e, deformities in the macroscopic contours of the electrode), and deformities in the small (the sharp protuberances that are associated with the surface microstructure). This section provides information on how to deal with such deformities when attempting to predict the occurrence of an electrostatic discharge. The main emphasis will be placed on deformities in the small, because these are the most difficult. At first glance, an electrode surface may appear to be smooth with a well defined radius of curvature, but a closer look under magnification shows tiny scratches, dents and protrusions. The question arises as to which radius of curvature (the radius of curvature seen without the magnification or the radius of curvature of the microscopic protrusions) should be used to calculate the electric field, i.e., should the electric field in the large be estimated or should the local electric field near the protrusions be estimated. This section attempts to answer that question. The answer depends on which kind of discharge mechanism will be in control. Therefore, the discussion of deformities in the small is combined with a brief discussion of several types of discharge mechanisms. This discussion is not an exhaustive review of discharge mechanisms and it does not provide all of the empirical data necessary to predict the occurrence of a breakdown. The discussion is only intended to give an idea as to what level of magnification must be looked at in order to predict a breakdown.

Deformities in the large can be treated in a rather simple way. For example, suppose the radius of curvature of an electrode surface is a smoothly varying function of position except near the apex where there is a deformity in the form of a small protrusion. Some examples in the appendix show electrodes with bumps on the end, and these examples indicate that Eq. (1.1) is still accurate providing that R is the radius of curvature at the end of the protrusion. To calculate V/E, the protrusion should be treated as part of the geometry and Eq. (1.1) used. As a second example, suppose the deformity is a dent near the apex. In this case the location of most intense electric field will probably be at the rim of the dent rather than at the apex. To calculate the most intense electric field, it is suggested that a worst case estimate be obtained by simulating the electrode with a pointed conductor having a radius of curvature at the apex equal to the maximum radius of curvature of the actual conductor. For either kind of deformity in the large, if the deformity is small compared to other dimensions of the geometry (including the spacing between electrode and grounded plane), it can obviously be neglected for the capacitance calculation.

As deformities are made smaller, by the time characteristic dimensions are on the order of tens of microns, they will begin to blend in with the microstructure of the surface. The effect that the microstructure has on the breakdown voltage depends on the discharge mechanism which, in turn, depends on the environment that the electrode is exposed to. Some discharge mechanisms are not yet well understood and are still an area of active research. A detailed discussion of what is known is beyond the scope of this report, but a few basic concepts are briefly discussed below.

## A. BREAKDOWN IN VACUUM

If the electrode is in a vacuum, there are several different mechanisms that can control the discharge as discussed below. In all cases, the breakdown voltage is very sensitive to the microstructure of the surface. If the surface is not perfectly clean, the breakdown voltage is also sensitive to contaminants such as oxides, adsorbed gases, etc. For a clean surface under ideal conditions, discharges are primarily controlled by the following mechanisms (see Ref. 5).

### 1. Field Emission at Cathode

If the gap between electrodes is less than 30 to 100 microns, and/or if the electric field at the cathode is much stronger than at the anode, a breakdown is controlled by field emission at the cathode. When the field emission current density reaches a critical value, joule heating produces an instability. For some materials the instability is caused by the softening of a protrusion in the microstructure so that it becomes (due to the force of the electric field) longer and sharper, producing even stronger fields and current densities. In other materials the instability is associated with a brittle fracture of a protrusion in the microstructure. In either case, the instability typically leads to a sequence of events (depending on the process, the sequence may begin with vaporization of cathode material, ejection of a fragment of material, or an emitter explosion which creates a plasma flare) that ultimately produces a breakdown. The critical current density (the value of the current density that initiates the breakdown process) is reproducible for a given material. As the current density increases to this critical value, the current is due to field emission, so that for a given material a well-defined electric field strength (given by the Fowler-Nordheim equation) corresponds to the critical current density. This implies that breakdown occurs when the electric field at the protrusion reaches a critical value. These values are known for many materials. Unfortunately, the relationship between the microscopic electric field at the protrusion and the macroscopic electric field is very sensitive to the microstructure, which is not usually known.

### 2. Breakdown Controlled by Conditions at Cathode and Anode

If the electric field at the anode is comparable to or larger than that at the cathode, and if the spacing between anode and cathode is more than 30 to 100 microns, breakdown is controlled by an interaction between cathode and anode. Electrons leaving the cathode due to field emission bombard the anode, vaporizing anode material. Electron bombardment of anode vapor causes ionization which produces an enhanced supply of electrons bombarding the anode to produce more vapor, and a runaway effect occurs. The process is further accelerated as positive ions approach the cathode and create a space charge which intensifies the electric field near the cathode and increases the electron emission current. Ion bombardment of the cathode creates another increase in the electron emission. When this interaction between cathode and anode takes place, breakdown will occur when the electric field at the cathode is lower than would be required if field emission alone (case "1" above) was controlling the process. But how much lower depends on the macroscopic field pattern as well as on the microstructure of the electrodes. Consequently, this case becomes difficult to treat quantitatively.

Under less ideal conditions, even if the electrodes are perfectly clean, discharges can be triggered by mechanisms not listed above. For example, a macroparticle can settle on an electrode, obtain some charge, and be repelled to the other electrode. If it impacts with enough energy, a discharge can be induced (Ref. 5). Another very important example is the sudden creation of a plasma. A discharge can occur at one location, creating a plasma which spreads to other locations and induces discharges at those locations (Ref. 7). Discharges through this mechanism can occur at very low voltages.

In summary, when electrodes are in an imperfect vacuum (e.g., the space environment), microscopic surface defects have a large influence on the breakdown voltage. But the microscopic structure is rarely known, and the discharge process is complicated by so many other variables that the occurrence of a discharge is difficult, if not impossible, to predict except in extreme cases. Reference 8 reports blow-off arcing at the several hundred volt level and explains that this phenomenon occurs in the space environment as well as in the laboratory. Reference 9 reports arcing at "greater than several hundred volts." Unless the reader has sufficient knowledge from his own resources to rule out the possibility of a discharge, it is suggested that it be assumed that a discharge is always possible when the medium separating the electrodes is the space environment and potentials reach several hundred volts or more. This is especially true if discharges can occur at other locations because a plasma can be created that induces a discharge at the location of interest (Ref. 7). The criteria for determining if an ESD hazard exists might be taken to be the calculated upper bound on the energy that could be released if a discharge should occur (see Section 3).

## B. BREAKDOWN IN SOLID DIELECTRIC

Breakdown through a dielectric due to a voltage applied to an electrode will always be a concern when high voltages are involved, because the function of a circuit element usually puts a limitation on how thick a dielectric can be. This situation is unavoidable. There are two other situations that are sometimes, if not most of the time, avoidable that can produce breakdowns. One situation occurs if a dielectric leaves too much of an electrode exposed so that an arc can follow along the surface of the dielectric (flashover). In order to determine the likelihood of this event, the dielectric cannot be treated as an infinite medium, and its surface must be included in the analysis. Strong surface charges are set up, which produce intense electric fields at the edges of the dielectric near the conductor, and the potential does not satisfy Laplace's equation at those locations. Consequently, the results of the previous sections of this report do not apply. The second situation is internal charging. This occurs when energetic charged particles from the spacecraft environment penetrate part way into the dielectric and get stuck there. Over a period of time they accumulate and create very intense electric fields which can lead to premature breakdown. Because this effect creates a space charge in the dielectric, the potential does not satisfy Laplace's equation. Therefore, the results of the previous sections of this report do not apply.

One thing that flashover and internal charging have in common is the fact that it is well known that these can be the effects that place the limits on a dielectric's ability to insulate unless precautions are taken to prevent their occurrence and such precautions should be taken whenever possible. Flashover can be prevented by covering exposed conducting surfaces with a dielectric. Internal charging can be reduced to low levels by mass shielding. Assuming that such precautions have been taken, the next discharge mechanism is a discharge through the dielectric (often call "treeing") due to the field created by the electrode. It is this process that will be considered here.

Like breakdown in a vacuum, which is described statistically (with the statistics controlled by the random microprotrusions, impurities, grain boundaries, etc., of the electrode surface), treeing is also a statistical phenomenon. However, authors of recent literature typically stress the importance of dielectric flaws rather than electrode microstructure on the statistical scatter (see, for example, Ref. 10). Examples of dielectric flaws are flaws in the crystal structure (if there is a crystal structure), small voids or cracks, and contaminants.

Basically, the process works as follows. It is initiated by the interaction of charged particles accelerated by the electric field with some weak point (a flaw) in the dielectric, producing a small region containing vaporized dielectric material. Since the region is now occupied by a vapor, the mean free path between collisions of charged particles with vapor molecules becomes long enough for ionization of the vapor molecules to occur, and an avalanche, the familiar Townsend discharge, begins. If conditions are right (the Paschen limit is reached), the discharge could become an arc, although this is not necessary in order for the breakdown process to continue. The bombardment by charged particles on the far end of the vapor-filled region causes more vaporization, and the region elongates, forming a "tree". By the time the tree reaches the opposite electrode, arcing between electrodes becomes possible.

Once the formation of a tree has been initiated, the breakdown process progresses easily, and the tree grows. The difficult part (although it is not difficult enough from our point of view) is getting it started. Flaws in the dielectric play a fundamental role in the process and as already stated, their importance rather than the importance of the electrode surface microstructure is typically emphasized in recent literature. This suggests that the electrode surface microstructure may not be an important influence. This idea is supported by the fact that in high voltage cables, trees often start from particles or voids that are completely surrounded by insulation material (Ref. 10). It is also supported by an experimental result described in Ref. 10. Two needles were embedded in a polyethylene dielectric and the voltage between them was increased until breakdown occurred. It was found that breakdown started at a beeswax-polymer interface, which is near the middle of one of the needles, instead of at the end of the needle where the electric field is 40 times as strong. Furthermore, the path of the breakdown ended on the shaft instead of the tip of the other needle. This suggests that breakdown is controlled more strongly by dielectric flaws than by local electric field enhancements. Still more support for the idea that local electric field enhancements are not strong controlling factors is provided by experimental results shown in Ref. 11. In this experiment, pins having various radii of curvature at the tip are embedded in a dielectric and the breakdown voltage is

measured. It was found that if the radius of curvature is made less than about 20 microns, further reductions in the radius of curvature did not affect the breakdown voltage.

The conclusion based on the above observations is that deformities in the electrode surface having characteristic dimensions of about 20 microns or less are probably not important and can be ignored. The reader should be aware that this conclusion is this author's speculation and not an indisputable fact. Treeing is not a well understood subject. The reader should also be aware that predictions of a breakdown are still statistical, even if the statistics are not controlled by the electrode surface microstructure, and the statistics depend on the length of time the electric field is applied as well as on other environmental and fabrication related factors.

## C. BREAKDOWN IN NEUTRAL GAS

When the Townsend criteria for breakdown, which is a theoretical derivation of Paschen's law, is applicable, the mechanism of breakdown in a gas is probably the only breakdown mechanism that is well understood. The basic idea is the following. An electron is emitted from the cathode due to field emission, ion bombardment, or other means. The electron collides with gas molecules creating ions and more free electrons. These free electrons are accelerated by the electric field and through collisions create still more ions and free electrons. This is a Townsend discharge. It is an avalanche effect with free electron density increasing as we move away from the cathode, but it can also be a stable (independent of time) discharge. To get the runaway effect (the arc) something else happens. The positive ions are attracted to the cathode and each ion that hits the cathode has some probability of freeing an electron due to secondary emission. If conditions are right, the ions resulting from one electron leaving the cathode will be in sufficient quantity to free more than one (on the average) electron through secondary emission. Therefore, each electron leaving the cathode will ultimately result in more than one electron leaving the cathode a short time later, and a runaway effect occurs. This is the arc, and the process described can be used to deduce Paschen's law. A quantitative treatment can be found in Ref. 12. When this process is occurring, the occurrence of breakdown is controlled by the number of gas ions ultimately produced by a single emitted electron. We would intuitively expect that an electric field will contribute to the avalanching of the ionization only if the spatial extent of the field is larger than some number of mean free paths. The local field enhancements (which have very small spatial extents) due to the electrode surface microstructure would not be expected to have an important effect.

The above statements suggest that the electrode surface microstructure is not important in the breakdown of a gas. This turns out to be true over the range of gas density where Paschen's law applies. Fortunately, this is a wide range of density. Unfortunately, it doesn't apply to all densities. At sufficiently high densities, the high local electric fields due to electrode imperfections, dust, etc., can lead to streamer-initiated breakdowns which result in Paschen's law not being satisfied (Ref. 13). Streamers are regions of low density and they behave similarly to the trees described in the discussion on solid dielectrics (Ref. 14). The effect of the streamer is to lower the breakdown voltage.

The conclusion from the above statements is that the protrusions found in the electrode surface microstructure are important for some gas densities and not for others. It would be helpful to know at what densities the transition occurs and quantitatively just how important the protrusions are when they are important. This information, applicable to air and SF6, can be found in Ref. 15. The data found in Figs. 5, 6, and 11 of Ref. 15 gives breakdown electric field strength in terms of surface protrusion characteristics. The data shows that the protrusions are only important, in the case of SF6, when the gas pressure times protrusion height is greater than about 40 bar-micron. So for a given pressure, protrusions with height less than 40 bar-micron divided by that pressure can be neglected under the conditions where the test data is valid. This only applies to pressures at or above those required for Paschen's law to be valid. At extremely low pressures, too low for Paschen's law to be valid, the electrode surface microstructure becomes important again because the discharge mechanisms applicable to a vacuum will begin to occur.

At pressures sufficiently high for the microstructure to be important, the data in Figs. 5, 6, and 11 of Ref. 15 can only be used if the maximum protrusion heights are known. This information is usually not known and breakdowns may have to be treated statistically. Even if the initial microstructure were known, it can be, depending on the initial state, significantly rougher after a breakdown occurs. If a worst case assumption is made for protrusion heights that takes into account the effects of arcing on surface roughening, and if the gas is air or SF6, the data found in Ref. 15 provides a method of predicting breakdowns if the electric field strength is known. This information can be calculated from the methods found in Sections 1 and 2 of this report.

# PART II - DERIVATIONS OF THE EQUATIONS

## SECTION 5

## PRELIMINARY DISCUSSION

The sections to follow provide mathematical derivations of the statements made in the first three sections of this report. Since all of the statements refer in some way or another to geometric properties of conductors or field patterns, it is best to begin the analysis by establishing a connection between geometric properties of the field and quantities that analytically represent the field. This connection is made in Sections 6 and 7, and provides a tool that will be used in later sections. Sections 8 through 12 each provide a derivation of a specific equation given in Part I. Section 13 provides a general description of the specific method, used in this report, of applying the least action principle to obtain a capacitance estimate. Section 14 derives the relatively simple capacitance estimate given as Eq. (3.2). Section 15 shows how a more accurate estimate can be obtained (involving a double integral) but this estimate takes more labor to numerically evaluate than Eq. (3.2). Algorithms for numerical evaluation are not provided and the reader will have to invent his own if he wishes to use those results.

Although it is not essential to the analyses that follow, various statements can be simplified if we are definite about the orientation of the coordinate system and the charge state of the conductor. The coordinate system to which all future discussions will refer is shown in Fig. 5.1. The phrases "left side" and "right side", which will be used frequently, refer to this figure. The conductor is assumed to be at a positive potential Vo relative to the grounded plane. $\vec{\varepsilon}$ represents the electric field at an arbitrary point in space while $\vec{E}$ represents the electric field on the Z axis so that $\vec{E}(Z) = \vec{\varepsilon}(0,0,Z)$. E or $\varepsilon$ without an arrow or subscript represents the magnitude of the electric field. $\phi$ represents the potential at an arbitrary point in space while V represents the potential on the Z axis so that $V(Z) = \phi(0,0,Z)$. Using these conventions, we don't use a negative sign when relating E to the derivative of V and we write

$$E = \frac{dV}{dZ} \quad . \tag{5.1}$$

L represents the distance between grounded plane and conductor. D is the distance between intercepts of the conductor with the Z axis. R(Z) is the radius of curvature, at the intersection with the Z axis, of the equipotential surface that intersects the axis at Z. $R_o = R(L)$ is the radius of curvature of the left apex of the conductor.

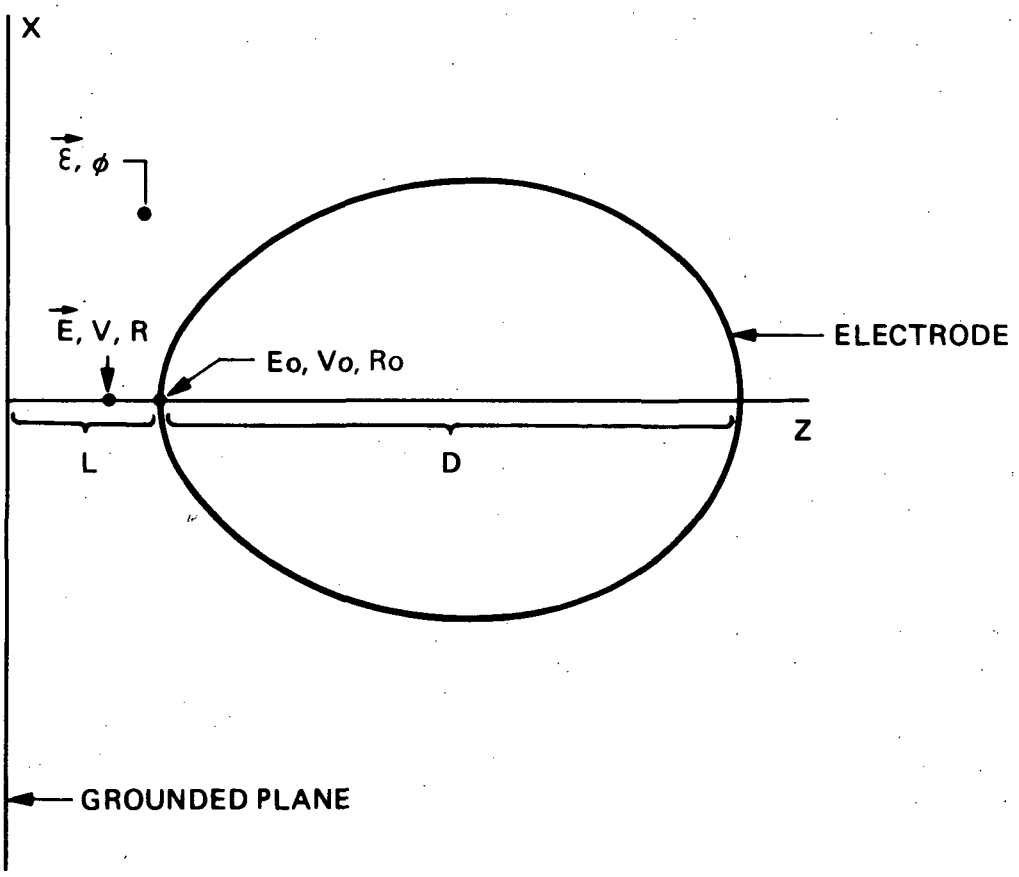


Fig. 5.1 Coordinate system orientation.

The Y axis is chosen to make a right-handed system. The electrode is at potential $V_0$ which is taken to be positive. $\vec{\varepsilon}$ and $\phi$ are the electric field and potential at an arbitrary point while $\vec{E}(Z) = \vec{\varepsilon}(0,0,Z)$ and $V(Z) = \phi(0,0,Z)$ are the electric field and potential on the Z axis. R(Z) is the radius of curvature, at the intersection with the Z axis, of the equipotential surface that intersects the axis at Z. $R_0 = R(L)$ is the radius of curvature of the apex of the electrode. $E_0 = E(L)$ is the magnitude of the electric field at the apex. D is the distance between intercepts.

## SECTION 6

## RADIUS OF CURVATURE OF EQUIPOTENTIAL SURFACE

An arbitrary equipotential surface intersects the XZ plane to define a curve in the plane. If we look at the portion of the curve that is on one side of the Z axis, the curve defines X as a function of Z and can be expressed as $X = f(Z)$. The equation for the radius of curvature at any given point on the curve can be found in any calculus text book and is

$$\frac{1}{R} = \frac{\left| \frac{d^2X}{dZ^2} \right|}{\left[ 1 + \left( \frac{dX}{dZ} \right)^2 \right]^{3/2}} . \tag{6.1}$$

The equation of the curve $X = f(Z)$ can also be expressed as $\phi(X,0,Z) = \text{constant}$ where the value of the constant is the potential at the point of interest. Implicit differentiation yields

$$\frac{\partial \phi(X,0,Z)}{\partial Z} + \frac{\partial \phi(X,0,Z)}{\partial X} \frac{dX}{dZ} = 0$$

$$\frac{\partial^2 \phi(X,0,Z)}{\partial Z^2} + \frac{2\partial^2 \phi(X,0,Z)}{\partial X \partial Z} \frac{dX}{dZ} + \frac{\partial^2 \phi(X,0,Z)}{\partial X^2} \left( \frac{dX}{dZ} \right)^2$$

$$+ \frac{\partial \phi(X,0,Z)}{\partial X} \frac{d^2X}{dZ^2} = 0.$$

The above equations can be solved for $dX/dZ$ and $d^2X/dZ^2$. Doing so and substituting into Eq. (6.1) gives

$$\frac{1}{R} = \frac{\left| \frac{\partial^2 \phi}{\partial Z^2} \left( \frac{\partial \phi}{\partial X} \right)^2 - 2 \frac{\partial^2 \phi}{\partial Z \partial X} \frac{\partial \phi}{\partial Z} \frac{\partial \phi}{\partial X} + \frac{\partial^2 \phi}{\partial X^2} \left( \frac{\partial \phi}{\partial Z} \right)^2 \right|}{\left[ \left( \frac{\partial \phi}{\partial X} \right)^2 + \left( \frac{\partial \phi}{\partial Z} \right)^2 \right]^{3/2}} . \tag{6.2}$$

Letting $\hat{e}_i$ represent the obvious unit vectors, the two dimensional del operator is defined by

$$\vec{\nabla}_{2D} = \hat{e}_1 \frac{\partial}{\partial X} + \hat{e}_3 \frac{\partial}{\partial Z} . \tag{6.3}$$

Eq. (6.2) can be rewritten as

$$\frac{1}{R} = \left| \vec{\nabla}_{2D} \cdot \left( \frac{\vec{\nabla}_{2D}\phi}{\left|\vec{\nabla}_{2D}\phi\right|} \right) \right| . \tag{6.4}$$

That the right side of Eq. (6.4) is the same as the right side of Eq. (6.2) can be verified by a brute force expansion using Eq. (6.3). The chain rule can be applied to the two dimensional del operator allowing Eq. (6.4) to be rewritten as

$$\frac{1}{R} = \left| \frac{\nabla^2_{2D}\phi}{\left|\vec{\nabla}_{2D}\phi\right|} - \frac{\vec{\nabla}_{2D}\,\phi \cdot \vec{\nabla}_{2D}\left|\vec{\nabla}_{2D}\phi\right|}{\left|\vec{\nabla}_{2D}\phi\right|^2} \right| . \tag{6.5}$$

Eqs. (6.4) and (6.5) apply to an arbitrary function $\phi$. The fact that it is a potential and satisfies Laplace's equation has never been used. We now make use of these facts. Letting $\vec{\nabla}$ represent the three dimensional del operator, the electric field is given by

$$\vec{\varepsilon} = - \vec{\nabla}\phi \ .$$

Since the electric field in the XZ plane has no Y component, $\partial\phi/\partial y = 0$ in the plane so

$$\vec{\varepsilon} = - \vec{\nabla}_{2D}\phi \quad \text{(in XZ plane)}$$

and Eq. (6.5) becomes

$$\frac{1}{R} = \left| - \frac{\vec{\nabla}_{2D} \cdot \vec{\varepsilon}}{\varepsilon} + \frac{\vec{\varepsilon} \cdot \vec{\nabla}_{2D}\varepsilon}{\varepsilon^2} \right| \tag{6.6}$$

If $\rho$ denotes radial distance from the Z axis, $\partial/\partial X = \partial/\partial\rho$ when the derivatives are evaluated in the XZ plane and $\varepsilon_\rho = \varepsilon_x$ in that plane so

$$\vec{\nabla}_{2D} \cdot \vec{\varepsilon} = \frac{\partial \varepsilon_\rho}{\partial \rho} + \frac{\partial \varepsilon_z}{\partial Z} \ . \tag{6.7}$$

In cylindrical coordinates, the equation $\vec{\nabla} \cdot \vec{\varepsilon} = 0$ becomes

$$\frac{\varepsilon_\rho}{\rho} + \frac{\partial \varepsilon_\rho}{\partial \rho} + \frac{\partial \varepsilon_z}{\partial Z} = 0. \tag{6.8}$$

The above two equations give

$$\vec{\nabla}_{2D} \cdot \vec{\varepsilon} = - \frac{\varepsilon_\rho}{\rho} \ . \tag{6.9}$$

Eq. (6.6) becomes

$$\frac{1}{R} = \frac{1}{\varepsilon} \left| \frac{\varepsilon_\rho}{\rho} + \frac{\vec{\varepsilon}}{\varepsilon} \cdot \vec{\nabla}_{2D}\varepsilon \right| . \tag{6.10}$$

Now let the point of evaluation move along the equipotential surface towards the Z axis. R becomes the radius of curvature evaluated on the Z axis while

$$\frac{\vec{\varepsilon}}{\varepsilon} \cdot \vec{\nabla}_{2D}\varepsilon \rightarrow -\hat{\varepsilon}_3 \cdot \vec{\nabla}_{2D}\varepsilon = -\frac{\partial \varepsilon}{\partial Z} .$$

Furthermore, $\varepsilon_\rho/\rho$ becomes an indeterminate form and l'Hôspital's Rule gives

$$\frac{\varepsilon_\rho}{\rho} \rightarrow \frac{\partial \varepsilon_\rho}{\partial \rho} . \tag{6.11}$$

Eq. (6.10) becomes

$$\frac{1}{R} = \lim_{\rho \to 0} \frac{1}{\varepsilon} \left| \frac{\partial \varepsilon_\rho}{\partial \rho} - \frac{\partial \varepsilon}{\partial Z} \right| \quad \text{(on axis)} . \tag{6.12}$$

Evaluation at $\rho = 0$ commutes with differentiation with respect to Z so

$$\frac{\partial \varepsilon}{\partial Z} \rightarrow \frac{\partial \varepsilon(0,0,Z)}{\partial Z} = -\frac{\partial \varepsilon_z(0,0,Z)}{\partial Z} . \tag{6.13}$$

Eqs. (6.8), (6.11), and (6.13) give

$$\frac{\partial \varepsilon_\rho}{\partial \rho} \rightarrow -\frac{1}{2} \frac{\partial \varepsilon_z}{\partial Z} = \frac{1}{2} \frac{\partial \varepsilon}{\partial Z} . \tag{6.14}$$

The expression for the radius of curvature now becomes

$$\frac{1}{R} = \frac{1}{2\varepsilon(0,0,Z)} \left| \frac{\partial \varepsilon(0,0,Z)}{\partial Z} \right| .$$

Since the electric field strength increases as we move towards the conductor, the absolute value sign can be dropped. Using the symbol $E(Z) = \varepsilon(0,0,Z)$, the equation finally becomes

$$\frac{1}{R(Z)} = \frac{1}{2E(Z)} \frac{dE(Z)}{dZ} . \tag{6.15}$$

## SECTION 7

## RADIUS OF CURVATURE OF ELECTRIC FIELD LINE

As was done in the previous section, we will look at curves in the XZ plane. This time the curves will represent electric field lines instead of equipotential surfaces.

Any calculus test book provides several expressions for the radius of curvature of a curve. One is given by Eq. (6.1). Another is (with Q denoting radius of curvature of an electric field line)

$$\frac{1}{Q} = \pm \frac{d\theta}{dS}$$

where dS is an element of arclength and $\theta$ is the angle between the tangent to the curve and the Z (in our case) axis. It is customary to use absolute values on the right side of the above equation but for our applications it will be useful to allow the radius of curvature to be positive under some conditions and negative under others.

The sign conventions that will be used are as follows. The radius of curvature of an electric field line will be positive if the field line bends towards the Z axis as we move away from the conductor, i.e., Q is positive if the field line is concave when viewed from the grounded plane. Otherwise Q is negative if it is finite. The arclength along a curve to a point on the curve will be taken to be increasing as the point moves away from the conductor. The unit tangent vector to the curve points in the direction of increasing arclength, i.e., it points away from the conductor. The unit tangent vector is in the direction of the electric field (since the conductor is assumed to be positively charged). $\theta$ is the angle between the unit tangent vector and $\hat{e}_3$. When all of these conventions are followed, it is easily seen that the correct sign for Q is given by

$$\frac{1}{Q} = \frac{d\theta}{dS} \quad . \tag{7.1}$$

To express Q in terms of electric field, note that $\tan\theta = \varepsilon_x/\varepsilon_z$ and

$$\frac{d\theta}{dS} = \frac{d\theta}{d(\tan\theta)} \frac{d(\tan\theta)}{dS} = \cos^2\theta \frac{d}{dS}\left(\frac{\varepsilon_x}{\varepsilon_z}\right)$$

$$= \frac{\varepsilon_z^2}{\varepsilon_x^2 + \varepsilon_z^2}\left[-\frac{\varepsilon_x}{\varepsilon_z^2}\frac{d\varepsilon_z}{dS} + \frac{1}{\varepsilon_z}\frac{d\varepsilon_x}{dS}\right]$$

or

$$\frac{d\theta}{dS} = \frac{1}{\varepsilon^2}\left[\frac{\varepsilon_z d\varepsilon_x}{dS} - \frac{\varepsilon_x d\varepsilon_z}{dS}\right] .$$

Note that

$$\frac{d}{dS} = \frac{dX}{dS}\ \frac{\partial}{\partial X} + \frac{dZ}{dS}\ \frac{\partial}{\partial Z} \ .$$

But dX/dS and dZ/dS are the components of the unit tangent vector which points in the direction of increasing arclength. This is the direction of the electric field so the unit tangent vector is $\vec{\varepsilon}/\varepsilon$ and

$$\frac{d}{dS} = \frac{\varepsilon_x}{\varepsilon}\ \frac{\partial}{\partial X} + \frac{\varepsilon_z}{\varepsilon}\ \frac{\partial}{\partial Z} \ .$$

This gives

$$\frac{d\theta}{dS} = \frac{1}{\varepsilon^3}\left[\varepsilon_x\varepsilon_z\ \frac{\partial\varepsilon_x}{\partial X} + \varepsilon_z{}^2\ \frac{\partial\varepsilon_x}{\partial Z} - \varepsilon_x{}^2\ \frac{\partial\varepsilon_z}{\partial X} - \varepsilon_x\varepsilon_z\ \frac{\partial\varepsilon_z}{\partial Z}\right] .$$

A brute force expansion of $\vec{\nabla}_{2D} \cdot (\varepsilon_x\ \hat{e}_3/\varepsilon - \varepsilon_z\ \hat{e}_1/\varepsilon)$ will verify that it is the same as the right side of the above equation. We now have

$$\frac{d\theta}{dS} = \vec{\nabla}_{2D} \cdot \left(\frac{\varepsilon_x \hat{e}_3}{\varepsilon} - \frac{\varepsilon_z \hat{e}_1}{\varepsilon}\right)$$

or

$$\frac{1}{Q} = \vec{\nabla}_{2D} \cdot \left(\frac{\varepsilon_x \hat{e}_3}{\varepsilon} - \frac{\varepsilon_z \hat{e}_1}{\varepsilon}\right) \qquad (7.2)$$

Eq. (7.2) could also have been deduced by making an analogy with Eq. (6.4). In Eq. (6.4) the operator $\vec{\nabla}_{2D}$ is operating on the unit vector (the electric field divided by its magnitude) that is perpendicular to the curve that the radius of curvature refers to. The same holds for Eq. (7.2). But the sign convention would have been less obvious if we used this analogy instead of starting with Eq. (7.1).

The fact that the electric field has a zero divergence and curl has not yet been used. As in Section 6, $\rho$ will denote radial distance from the Z axis. In analogy with Eq. (6.7) we write Eq. (7.2) as

$$\frac{1}{Q} = \frac{\partial}{\partial Z}\left(\frac{\varepsilon_\rho}{\varepsilon}\right) - \frac{\partial}{\partial \rho}\left(\frac{\varepsilon_z}{\varepsilon}\right) .$$

Expanding and using the fact that the three dimensional curl of $\vec{\varepsilon}$ is zero produces

$$\frac{1}{Q} = \frac{\varepsilon_z}{\varepsilon^2}\ \frac{\partial\varepsilon}{\partial\rho} - \frac{\varepsilon_\rho}{\varepsilon^2}\ \frac{\partial\varepsilon}{\partial Z} \ . \qquad (7.3)$$

In the applications to follow, the behavior of the radius of curvature Q will be of concern only in the immediate vicinity of the Z axis. But as the point of evaluation approaches the Z axis, Q will become infinite (the electric field line is straight on the Z axis). Therefore, the best way to describe the behavior of Q in this limit is to compare its behavior to $\rho$. This motivates us to define T by

$$T = \lim_{\rho \to 0} \frac{1}{\rho} \frac{1}{Q} . \tag{7.4}$$

Once T has been solved, the behavior of Q is given by

$$\frac{1}{Q} \to T\rho . \tag{7.5}$$

If the right side of Eq. (7.3) is used to replace 1/Q in Eq. (7.4), the resulting expression can be written as

$$T = \lim_{\rho \to 0} \left[ \frac{\varepsilon_z}{\varepsilon^2} \left( \frac{1}{\rho} \frac{\partial \varepsilon}{\partial \rho} \right) - \frac{1}{\varepsilon^2} \left( \frac{\varepsilon_\rho}{\rho} \right) \frac{\partial \varepsilon}{\partial Z} \right] .$$

The quantities in parentheses are indeterminate forms and l'Hôspital's Rule gives

$$T = \lim_{\rho \to 0} \left[ -\frac{1}{\varepsilon} \frac{\partial^2 \varepsilon}{\partial \rho^2} - \frac{1}{\varepsilon^2} \frac{\partial \varepsilon_\rho}{\partial \rho} \frac{\partial \varepsilon}{\partial Z} \right]$$

or, using Eq. (6.14)

$$T = \lim_{\rho \to 0} \left[ -\frac{1}{\varepsilon} \frac{\partial^2 \varepsilon}{\partial \rho^2} - \frac{1}{2\varepsilon^2} \left( \frac{\partial \varepsilon}{\partial Z} \right)^2 \right] . \tag{7.6}$$

To get another expression for $\partial^2\varepsilon/\partial\rho^2$, note that

$$\frac{\partial \varepsilon}{\partial \rho} = \frac{\partial}{\partial \rho} \left[ \varepsilon_\rho^2 + \varepsilon_z^2 \right]^{1/2} = \frac{\varepsilon_\rho}{\varepsilon} \frac{\partial \varepsilon_\rho}{\partial \rho} + \frac{\varepsilon_z}{\varepsilon} \frac{\partial \varepsilon_z}{\partial \rho}$$

so

$$\frac{\partial^2 \varepsilon}{\partial \rho^2} \to \frac{1}{\rho} \frac{\partial \varepsilon}{\partial \rho} = \frac{1}{\varepsilon} \frac{\varepsilon_\rho}{\rho} \frac{\partial \varepsilon_\rho}{\partial \rho} + \frac{\varepsilon_z}{\varepsilon} \frac{1}{\rho} \frac{\partial \varepsilon_z}{\partial \rho} \to \frac{1}{\varepsilon} \left( \frac{\partial \varepsilon_\rho}{\partial \rho} \right)^2 + \frac{\varepsilon_z}{\varepsilon} \frac{\partial^2 \varepsilon_z}{\partial \rho^2} .$$

Using Eq. (6.14) this becomes

$$\frac{\partial^2 \varepsilon}{\partial \rho^2} \to \frac{1}{4\varepsilon} \left( \frac{\partial \varepsilon}{\partial Z} \right)^2 + \frac{\varepsilon_z}{\varepsilon} \frac{\partial^2 \varepsilon_z}{\partial \rho^2} .$$

But rectangular components of the electric field satisfy Laplace's equation (which is easily verified by writing Laplace's equation for the potential and differentiating both sides with respect to an arbitrary rectangular coordinate and noting that the derivatives commute) and this leads to

$$\frac{\partial^2 \varepsilon_z}{\partial Z^2} = -\frac{1}{\rho}\frac{\partial \varepsilon_z}{\partial \rho} - \frac{\partial^2 \varepsilon_z}{\partial \rho^2} \rightarrow -2\frac{\partial^2 \varepsilon_z}{\partial \rho^2}$$

or

$$\frac{\partial^2 \varepsilon_z}{\partial \rho^2} \rightarrow -\frac{1}{2}\frac{\partial^2 \varepsilon_z}{\partial Z^2}$$

so that

$$\frac{\partial^2 \varepsilon}{\partial \rho^2} \rightarrow \frac{1}{4\varepsilon}\left(\frac{\partial \varepsilon}{\partial Z}\right)^2 - \frac{\varepsilon_z}{2\varepsilon}\frac{\partial^2 \varepsilon_z}{\partial Z^2} \rightarrow \frac{1}{4\varepsilon}\left(\frac{\partial \varepsilon}{\partial Z}\right)^2 - \frac{1}{2}\frac{\partial^2 \varepsilon}{\partial Z^2}.$$

Eq. (7.6) now becomes

$$T = \lim_{\rho \to 0}\left[-\frac{3}{4\varepsilon^2}\left(\frac{\partial \varepsilon}{\partial Z}\right)^2 + \frac{1}{2\varepsilon}\frac{\partial^2 \varepsilon}{\partial Z^2}\right]$$

or

$$T = -\frac{3}{4E^2}\left(\frac{dE}{dZ}\right)^2 + \frac{1}{2E}\frac{\partial^2 E}{\partial Z^2}. \tag{7.7}$$

Differentiating Eq. (6.15) produces

$$\frac{d^2E}{dZ^2} = \frac{2}{R}\frac{dE}{dZ} - \frac{2E}{R^2}\frac{dR}{dZ} = \frac{4E}{R^2} - \frac{2E}{R^2}\frac{dR}{dZ}. \tag{7.8}$$

Using Eq. (6.15) and (7.8) to substitute into Eq. (7.7) produces

$$T = -\frac{1}{R^2}\left(1 + \frac{dR}{dZ}\right). \tag{7.9}$$

The behavior of the radius of curvature of the electric field line in the vicinity of the Z axis is related to $\rho$ and the radius of curvature of the equipotential surface passing through the same point by Eqs. (7.5) and (7.9) which give

$$\frac{1}{Q} \rightarrow -\frac{\rho}{R^2}\left(1 + \frac{dR}{dZ}\right). \tag{7.10}$$

## SECTION 8

## DERIVATION OF EQUATION 1.1

As explained in Section 1, Eq. (1.1) can be expected to provide an approximation for the potential over the electric field at the apex of an arbitrary equipotential surface (which includes the surface of the conductor) if it can be shown that K, defined by Eq. (1.3), approaches 2/3 as the equipotential surface used to define K approaches the grounded plane.

To show that $K \to 2/3$, we associate the quantities on the right side of Eq. (1.3) with an equipotential surface that intersects the Z axis at some arbitrary point Z. To make this association we simply replace L with Z and show all of the other quantities to be functions of Z so that Eq. (1.3) becomes

$$K(Z) = \frac{(ZE(Z) - V(Z))}{V(Z)} \frac{R(Z)}{Z} \quad . \tag{8.1}$$

The objective is to show that the right side of Eq. (8.1) goes to 2/3 as $Z \to 0$.

Eq. (6.15) can be used to eliminate R(Z) in Eq. (8.1) to give

$$\frac{K}{2} = \frac{\left(\frac{E}{V} - \frac{1}{Z}\right) E}{E'} \tag{8.2}$$

where prime denotes differentiation with respect to Z. For notational brevity, the Z dependence of the various quantities is not explicitly shown but is implied. It is assumed that the electric field varies smoothly with Z so all odd derivatives of E go to zero as Z goes to zero. This means that the right side of Eq. (8.2) is an indeterminate form. But the numerator is the difference of two terms that each diverge so l'Hospital's rule should not be applied yet (the limit of the difference is not equal to the difference in the limits). First rewrite the equation as

$$\frac{K}{2} = \frac{ZE^2 - VE}{ZVE'} \quad .$$

One application of l'Hospital's rule gives (using Eq. (5.1))

$$\lim_{Z \to 0} \frac{K}{2} = \frac{2ZEE' - VE'}{VE' + ZEE' + ZVE''} \quad .$$

This is still an indeterminate form. Two more applications of l' Hospital's rule together with Eq. (5.1) is needed to remove the indeterminacy . After this is done, setting odd derivatives of E equal to zero yields the desired result

$$\lim_{Z \to 0} \frac{K}{2} = \frac{1}{3}$$

or $K \to 2/3$.

As an incidental point, Eq. (1.1) can also be found in Ref. 11. The author of that reference discovered the equation by curve fitting to computer generated results and that is exactly how the author of this report made the same discovery. Reference 11 analytically shows that Eq. (1.1) is an approximation for needle electrodes by taking a specific analytic solution to a boundary value problem and noting that Eq. (1.1) is an approximation to that solution. The derivation is only valid for a special case although the conclusion is more general. The derivation given in this report applies to all possible solutions to Laplace's equation having the required symmetry.

## SECTION 9

## DERIVATION OF INEQUALITY 1.4

To get one side of Inequality (1.4), note that if the equipotential surfaces are convex when viewed from the grounded plane, the electric field strength is an increasing function of Z. Therefore, $E_o = E(L) \geq E(Z)$ for $0 \leq Z \leq L$ which implies

$$\int_0^L E_o dZ \geq \int_0^L E(Z)dZ$$

or

$$V_o \leq E_o L$$

or

$$\frac{V_o}{E_o} \leq L.$$

To get the other side of the inequality, assume that the electric field lines that are in a neighborhood of the Z axis bend towards the Z axis as the point of observation moves from the conductor to the grounded plane. From the sign convention used in Section 7, this is equivalent to saying that Q is positive at points sufficiently close to the axis. This implies that the right side of Eq. (7.10) is positive which implies

$$\frac{dR}{dZ} < -1 \qquad 0 < Z < L$$

Which implies

$$\int_Z^L R'(X)\, dX < -\int_Z^L dX$$

or

$$R(L) - R(Z) < -(L - Z)$$

or

$$R(Z) > L - Z + R(L) = L - Z + R_o \ .$$

But

$$R(Z) = \frac{2E(Z)}{E'(Z)}$$

so

$$\frac{E'(Z)}{2E(Z)} < \frac{1}{L + R_o - Z} \quad .$$

This gives

$$\int_Z^L \frac{E'(X)}{2E(X)}\, dX < \int_Z^L \frac{dX}{L + R_o - X}$$

or

$$\frac{1}{2} \ln\left(\frac{E_o}{E(Z)}\right) < \ln\left(\frac{Z + R_o}{R_o}\right)$$

or

$$E(Z) > \frac{R_o^2 E_o}{(Z + R_o)^2} \quad .$$

Integrating both sides of the above inequality between 0 and L produces the desired result

$$\frac{V_o}{E_o} > \frac{LR_o}{L + R_o} \quad .$$

## SECTION 10

## DERIVATION OF EQUATION 2.1

The model field is defined to satisfy Eq. (1.1) when the quantities in the equation refer to an arbitrary equipotential surface. Using the present symbolism that is appropriate for an arbitrary equipotential surface, the equation is written as

$$\frac{V(Z)}{E(Z)} = \frac{ZR(Z)}{\frac{2}{3}Z + R(Z)} \quad . \tag{10.1}$$

Using Eq. (6.15) to replace R gives

$$V = \frac{ZE^2}{\frac{1}{3}ZE' + E} \quad .$$

Differentiating the above equation and using $E = dV/dZ$ and doing some rearranging of terms yields

$$\frac{5}{3}Z^2\frac{E'^2}{E^2} + Z\frac{E'}{E} - Z^2\frac{E''}{E} = 0 \quad . \tag{10.2}$$

Note

$$\frac{Z}{E}\frac{dE}{dZ} = \frac{d\ \ln E}{d\ \ln Z} \tag{10.3}$$

and

$$\frac{d^2\ \ln E}{d(\ln Z)^2} = \frac{d}{d\ \ln Z}\left(\frac{Z}{E}\frac{dE}{dZ}\right) = \frac{dZ}{d\ \ln Z}\frac{d}{dZ}\left(\frac{Z}{E}\frac{dE}{dZ}\right)$$

$$= \frac{Z}{E}\frac{dE}{dZ} - \frac{Z^2}{E^2}\left(\frac{dE}{dZ}\right)^2 + \frac{Z^2}{E}\frac{d^2E}{dZ^2} = \frac{d\ \ln E}{d\ \ln Z} - \left(\frac{d\ \ln E}{d\ \ln Z}\right)^2 + \frac{Z^2}{E}\frac{d^2E}{dZ^2}$$

or

$$\frac{Z^2}{E}\frac{d^2E}{dZ^2} = \frac{d^2\ln E}{d(\ln Z)^2} - \frac{d\ \ln E}{d\ \ln Z} + \left(\frac{d\ \ln E}{d\ \ln Z}\right)^2 \quad . \tag{10.4}$$

Putting Eqs. (10.3) and (10.4) into Eq. (10.2) yields

$$\frac{2}{3}\left(\frac{d\ \ln E}{d\ \ln Z}\right)^2 + 2\frac{d\ \ln E}{d\ \ln Z} - \frac{d^2\ \ln E}{d(\ln Z)^2} = 0 \quad .$$

If we make the change in variables

$$u = \frac{d\ \ln\ (E/E_o)}{d\ \ln\ (Z/L)} \quad \text{and} \quad v = \ln\ (Z/L) \tag{10.5}$$

the equation becomes

$$\frac{du}{dv} = \frac{2}{3}\ u^2 + 2u$$

or

$$dv = \frac{du}{\frac{2}{3}\ u^2 + 2u}\ .$$

This equation can be integrated to give

$$v = \ln \left[ \frac{2 + \frac{2}{3}\ u}{u} \right]^{-1/2} + C \tag{10.6}$$

for some constant C. To evaluate this constant, let $Z \to L$. Then $v = \ln (Z/L) \to 0$. Note

$$u = \frac{d\ \ln\ (E/E_o)}{d\ \ln\ (Z/L)} = \frac{Z}{E}\ \frac{dE}{dZ}\ . \tag{10.7}$$

From Eq. (6.15) we have $u = 2Z/R$ which implies $u \to 2L/R_o$ as $Z \to L$. The integration constant must satisfy

$$0 = \ln \left[ \frac{2 + \frac{2}{3}\ (\frac{2L}{R_o})}{\frac{2L}{R_o}} \right]^{-1/2} + C.$$

Substituting for C in Eq. (10.6) gives

$$v = \ln \left[ \frac{R_o + \frac{2}{3}\ L}{L}\ \frac{u}{2 + \frac{2}{3}\ u} \right]^{1/2}\ .$$

But $v = \ln (Z/L)$ so the equation becomes

$$\frac{Z}{L} = \left[ \frac{R_o + \frac{2}{3}\ L}{L}\ \frac{u}{2 + \frac{2}{3}\ u} \right]^{1/2}$$

which can be written as

$$u = \frac{2Z^2}{R_o L - \frac{2}{3}(Z^2 - L^2)} .$$

Using Eq. (10.7) this becomes

$$\frac{dE}{E} = \frac{ZdZ}{\left(\frac{1}{2} R_o L + \frac{1}{3} L^2\right) - \frac{1}{3} Z^2}$$

which can be integrated from Z = L to an arbitrary value to give

$$E = E_o \left[ \frac{\frac{3}{2} R_o L}{\frac{3}{2} R_o L + L^2 - Z^2} \right]^{3/2} . \qquad (10.8)$$

Eq. (10.8) would be more convenient if it were expressed in terms of $V_o$ instead of $E_o$. The two can be related by integrating Eq. (10.8) between 0 and L, but a faster way is to use Eq. (10.1) evaluated at Z = L. Doing this and substituting for $E_o$ in Eq. (10.8) yields

$$E(Z) = \frac{V_o \left(L + \frac{3}{2} R_o\right) \left[\frac{3}{2} L R_o\right]^{1/2}}{\left[L^2 + \frac{3}{2} R_o L - Z^2\right]^{3/2}} \qquad (10.9)$$

or

$$E(Z) = \frac{V_o M^2 [M^2 - L^2]^{1/2}}{L [M^2 - Z^2]^{3/2}} \qquad (10.10)$$

where M is defined by

$$M^2 = L^2 + \frac{3}{2} L R_o . \qquad (10.11)$$

The potential is obtained by integrating Eq. (10.10). The result is

$$V(Z) = \frac{V_o}{L} [M^2 - L^2]^{1/2} \frac{Z}{[M^2 - Z^2]^{1/2}} \qquad (10.12)$$

which is Eq. (2.1). The radius of curvature can also be solved as a function of Z. Eq. (6.15) together with Eq. (10.10) yield

$$R(Z) = \frac{2}{3} \frac{M^2 - Z^2}{Z} \qquad (10.13)$$

or, equivalently,

$$Z^2 + \frac{3}{2} ZR(Z) = \text{constant} = M^2 \quad .$$

As an incidental point, the electric field strength at the grounded plane is obtained by letting Z = 0 in Eq. (10.10) to get

$$E(0) = \frac{V_o}{L} \frac{[M^2 - L^2]^{1/2}}{M} \quad .$$

It can be related to the electric field strength at the apex by first letting Z = L in Eq. (10.10) to get

$$E_o = \frac{V_o M^2}{L (M^2 - L^2)}$$

and then combine equations to get

$$\frac{E_o}{E(0)} = \frac{M^3}{[M^2 - L^2]^{3/2}} = \left[ \frac{2}{3} \frac{L}{R_o} + 1 \right]^{3/2} \quad . \qquad (10.14)$$

Eq. (10.14) provides an estimate of the uniformity of the electric field strength.

## SECTION 11

## DERIVATION OF EQUATION 2.4

It was found in the previous section that the potential on the Z axis for the model field satisfies Eq. (10.12). To evaluate the potential at points off of the axis, we use the procedure presented on page 91 of Ref. 16. The potential can be represented, in a suitably restricted domain, by the expansion

$$\phi = \sum_{\ell=0}^{\infty} A_\ell r^\ell P_\ell(\cos\theta) \quad . \tag{11.1}$$

$\theta$ is the angle between the positive Z axis and the vector from the origin to the point of evaluation. The distance from the origin to the point of evaluation is r. The Ps are the Legendre polynomials and the As are unknown constants that have to be determined. Only positive powers of r are used in Eq. (11.1) because it is intended that the series represent the potential inside some spherical region centered at the origin (actually, Eq. (11.1) is only good for the right half of this spherical region if the physical system consists of an electrode and grounded plane rather than two electrodes). The radius of this spherical region depends on the convergence properties that the series will have. It will turn out that the solution will be valid only for $r < M$. This is not surprising because if $r \to M$ along the Z axis, Eq. (10.12) shows a singularity in the potential.

On the Z axis, $\cos\theta = 1$ and Eq. (11.1) becomes

$$\phi(0,0,Z) = \sum_{\ell=0}^{\infty} A_\ell r^\ell = \sum_{\ell=0}^{\infty} A_\ell Z^\ell \quad .$$

But the potential on the axis is given by Eq. (10.12) so the A's must satisfy

$$\sum_{\ell=0}^{\infty} A_\ell Z^\ell = \frac{V_o}{L} \left[M^2 - L^2\right]^{1/2} \frac{Z}{\left[M^2 - Z^2\right]^{1/2}} \quad . \tag{11.2}$$

The next step is to expand the right side of Eq. (11.2) as a power series in Z. The general form of the binomial expansion can be written as (Ref. 17)

$$(1 + X)^{\beta} = \sum_{n=0}^{\infty} \frac{\beta! X^n}{n!(\beta - n)!}$$

which gives

$$(1 + X)^{-1/2} = \sum_{n=0}^{\infty} \frac{(-1/2)! X^n}{n!(-1/2 - n)!} \quad . \tag{11.3}$$

From page 453 of Ref. 17 we have

$$(-1/2)! = \pi^{1/2}$$

and from page 457 of Ref. 17 we have

$$(-1/2 - n)!(n - 1/2)! = (-1)^n\pi$$

or

$$(-1/2 - n)! = \frac{(-1)^n\pi}{(n - 1/2)!}$$

so Eq. (11.3) becomes

$$(1 + X)^{-1/2} = \sum_{n=0}^{\infty} \frac{\pi^{1/2}X^n(n - 1/2)!}{n!(-1)^n\pi} = 1 + \pi^{-1/2} \sum_{n=1}^{\infty} (-1)^n \frac{(n - 1/2)!\, X^n}{n!} .$$

Note that

$$(m + 1/2)! = \frac{(2m + 1)}{2}\cdots\left(\frac{3}{2}\right)\left(\frac{1}{2}\right)\left(-\frac{1}{2}\right)! = \frac{(2m + 1)}{2}\cdots\left(\frac{3}{2}\right)\left(\frac{1}{2}\right)\pi^{1/2}$$

$$= \pi^{1/2}\,\frac{(2m + 2)!}{2^{2m+2}(m + 1)!} = \frac{\pi^{1/2}(2m + 1)!}{2^{2m + 1}\,m!} \qquad m \geq 0$$

so

$$(n - 1/2)! = \frac{\pi^{1/2}(2n - 1)!}{2^{2n - 1}(n - 1)!} \qquad n \geq 1$$

and we finally get

$$(1 + X)^{-1/2} = 1 + \sum_{n=1}^{\infty} \frac{(-1)^n\,(2n - 1)!}{2^{2n - 1}\,n!\,(n - 1)!}\, X^n .$$

Applying the above result to the right side of Eq. (11.2) gives

$$\frac{V_o}{L}\,\frac{[M^2 - L^2]^{1/2}Z}{[M^2 - Z^2]^{1/2}}$$

$$= \frac{V_o}{L}\,[M^2 - L^2]^{1/2} \cdot \left\{\frac{Z}{M} + \sum_{n=1}^{\infty} \frac{(2n - 1)!}{2^{2n - 1}n!(n - 1)!}\left(\frac{Z}{M}\right)^{2n + 1}\right\} . \qquad (11.4)$$

Replacing the right side of Eq. (11.2) with the right side of Eq. (11.4) produces an equality between two power series in Z and this is used to solve for the coefficients $A_\ell$ (the coefficients with an even subscript will be zero). After the coefficients have been solved, the potential at an arbitrary point can be obtained from Eq. (11.1). The result is Eq. (2.4) (note that An in Eq. (2.4) is not the same as it is in Eq. (11.1)).

## SECTION 12

## DERIVATION OF EQUATION 2.5

We will begin this section by temporarily forgetting about the physical system that we have been working with and investigate an entirely new boundary value problem that will appear to be totally unrelated to the original problem. The reason for doing this is that there is a general method, described later in this section, for constructing solutions to Laplace's equation out of other solutions. The solution to the boundary value problem that is described below will be used to construct the solution to our original problem.

In this new problem, the grounded plane is oriented in the coordinate system as before but not all of the plane is grounded. A circular section of radius M is electrically isolated from the rest of the plane and held at a potential $V_a$. The remainder of the plane is grounded. There are no other boundary surfaces (i.e., no electrode) in this problem except the surface at infinity which is at zero potential. Let $\psi$ denote the potential, at an arbitrary point to the right of the plane, created by this system. The first objective is to solve for $\psi$.

Let $G(\vec{X}, \vec{X}')$ denote the Green's function for this system (a general discussion of Green's functions can be found in Ref. 16 or 18). $\psi$ can be expressed in terms of G by

$$\psi(\vec{X}) = -\frac{V_a}{4\pi} \int \vec{\nabla}' G(\vec{X}, \vec{X}') \cdot d\vec{a}' \qquad (12.1)$$

where the integral is a surface integral and the surface of integration is the circular region of the plane that is at potential $V_a$. The Green's function can be thought of as the potential, measured at a point $\vec{X}$, that results when a unit point charge is placed at $\vec{X}'$ and all boundary surfaces are grounded. G, in this case, is easily solved using the method of images. Suppose a point charge q is placed at some location $\vec{X}'$. This location is on the right side of the plane but is otherwise arbitrary. Let $\vec{X}' = X'\hat{e}_1 + Y'\hat{e}_2 + Z'\hat{e}_3$. An image charge -q will be located at $X'\hat{e}_1 + Y'\hat{e}_2 - Z'\hat{e}_3$. The potential at a point $\vec{X}$ is

$$\frac{q}{\left|\vec{X} - \left(X'\hat{e}_1 + Y'\hat{e}_2 + Z'\hat{e}_3\right)\right|} - \frac{q}{\left|\vec{X} - \left(X'\hat{e}_1 + Y'\hat{e}_2 - Z'\hat{e}_3\right)\right|} .$$

We are presently using the cgs system of units but the final result, which will relate potential at a point in space to potential on a boundary surface, will be independent of the system of units used. The Green's function is given by

$$G(\vec{X}, \vec{X}') = \frac{1}{\left|\vec{X} - \left(X'\hat{e}_1 + Y'\hat{e}_2 + Z'\hat{e}_3\right)\right|} - \frac{1}{\left|\vec{X} - \left(X'\hat{e}_1 + Y'\hat{e}_2 - Z'\hat{e}_3\right)\right|} . \qquad (12.2)$$

Note that

$$\vec{\nabla}' G(\vec{X}, \vec{X}') \cdot d\vec{a}' = \frac{\partial G}{\partial Z'}(\vec{X}, \vec{X}')\, dX'dY'. \tag{12.3}$$

Using $|\vec{X} - (X'\hat{e}_1 + Y'\hat{e}_2 \pm Z'\hat{e}_3)| = [(X - X')^2 + (Y - Y')^2 + (Z \mp Z')^2]^{1/2}$, the derivative of Eq. (12.2) can be calculated directly and the result is

$$\left.\frac{\partial G}{\partial Z'}\right|_{Z'=0} = \frac{-2Z}{\left[(X - X')^2 + (Y - Y')^2 + (Z)^2\right]^{3/2}} . \tag{12.4}$$

Using Eqs. (12.1), (12.3), and (12.4) we get

$$\psi(\vec{X}) = \frac{V_a Z}{2\pi} \int_{(X')^2+(Y')^2<M^2} [(X - X')^2 + (Y - Y')^2 + (Z)^2]^{-3/2}\, dX'dY' . \tag{12.5}$$

The usefulness of Eq. (12.5) will begin to become visible if it is evaluated on the Z axis. The integral can be evaluated directly and the result is

$$\psi(0,0,Z) = V_a - \frac{V_a Z}{[M^2 + Z^2]^{1/2}} . \tag{12.6}$$

Notice the similarity between Eq. (12.6) and Eq. (2.1). Aside from an additive constant and a proportionality constant, they differ only in the sign in front of the $Z^2$. If the potentials $\phi$ (the solution to the original boundary value problem) and $\psi$ (given by Eq. (12.5)) were equal on the Z axis (which of course they are not), they would be equal everywhere inside some sphere with a radius that depends on the convergence properties of the expression for $\psi$. If we could simply replace Z with iZ (where i is the imaginary number) in Eq. (12.5) and adjust additive constants and proportionality constants, we would have the solution that we are looking for. It turns out that we can follow a procedure that is almost that simple by using the following theorems.

Theorem 1

Let f(X,Y,Z) be defined when each argument X, Y, and Z are complex numbers. Assume that f is analytic in each argument when

$$|X|^2 + |Y|^2 + |Z|^2 < M^2 \tag{12.7}$$

for some real $M > 0$. Assume also that f satisfies Laplace's equation when X, Y, and Z are real and satisfy Eq. (12.7). Then f satisfies Laplace's equation for all complex X, Y, Z satisfying Eq. (12.7).

Proof

Define g by

$$g(X,Y,Z) = \nabla^2 f(X,Y,Z) = \frac{\partial^2 f}{\partial X^2} + \frac{\partial^2 f}{\partial Y^2} + \frac{\partial^2 f}{\partial Z^2} .$$

Since derivatives of analytic functions are analytic (Ref. 19), g is analytic for all X, Y, Z satisfying Eq. (12.7). By hypothesis, $g(X,Y,Z) = 0$ when X, Y, Z are real and satisfy Eq. (12.7). Let $Y_o$ and $Z_o$ be real and satisfy

$$Y_o^2 + Z_o^2 < M^2 .$$

Then $g(X,Y_o,Z_o)$ is analytic in X when X is complex and satisfies

$$|X|^2 < M^2 - Y_o^2 - Z_o^2 \qquad (12.8)$$

and it is zero when X is real and satisfies Eq. (12.8). From the fundamental theorem on analytic continuation (page 152, Ref. 19) it follows that $g(X,Y_o,Z_o) = 0$ for all complex X satisfying Eq. (12.8). If we now regard X as fixed and repeat this line of reasoning for the remaining coordinates, we get $g(X,Y,Z) = 0$ for all X, Y, Z satisfying Eq. (12.7) which proves the theorem.

Theorem 2

Given the same hypothesis as Theorem 1, then the real part and imaginary part of f(iX,iY,iZ) each satisfy Laplace's equation when X, Y, and Z are real and satisfy Eq. (12.7).

Proof

A trivial application of Theorem 1 and the chain rule will show that

$$\nabla^2 f(iX,iY,iZ) = 0 \qquad (12.9)$$

for any X, Y, Z satisfying Eq. (12.7) and in particular for real X, Y, Z satisfying Eq. (12.7). The real part and imaginary part of the left side of Eq. (12.9) are individually zero. When the coordinates are real the Laplacian of the real (imaginary) part is the real (imaginary) part of the Laplacian.

The above theorem can be loosely summarized as follows. If f(X,Y,Z) satisfies Laplace's equation when the coordinates are real and if the function is mathematically defined and analytic when the coordinates are each regarded as complex numbers, then the functions Re f(iX,iY,iZ) and Im f(iX,iY,iZ), which are real functions of the real coordinates X, Y, Z, also satisfy Laplace's equation. This interpretation is loose only because the domains haven't been

properly specified. But this turns out to be an important consideration. Two functions, f1(X,Y,Z) and f2(X,Y,Z) may be equal when the arguments are real but not equal when the arguments are complex. One function may be analytic over the required domain and the other not. Although the two functions are indistinguishable when the arguments are real, the theorem does not apply to both functions. It applies only to the one that is analytic over the required domain.

One systematic procedure for constructing a function that satisfies the hypothesis of Theorem 2 out of a function that is originally defined only when the arguments are real is to expand the original function in a Taylor series that is valid for real arguments. Then let this series define the function for complex values of the arguments. The function defined by the series will be analytic on a domain that depends on the radius of convergence of the series. If necessary, it may be possible to enlarge the domain using analytic continuation. An alternate approach is trial and error. Find different ways of expressing the given function, that are equivalent when the arguments are real, until an expression is obtained that is recognized as being mathematically defined and analytic when the arguments are complex. If such an expression is obtained, it will be equal to the function defined by the series just described.

Fortunately, in the case of Eq. (12.5), it isn't necessary to use the series method or to find new ways to express it so that the new expression contains functions that are defined in the complex plane. The quantities contained in Eq. (12.5) already have a natural interpretation in the complex plane. The only thing that must be decided is what determination to use for the square root function. Let us use the principal determination and see if it produces the solution we want.

One of the integrations in Eq. (12.5) can be performed. It is convenient to make the following change in variables, where all coordinates are regarded as real for the time being.

$$r = (X^2 + Y^2 + Z^2)^{1/2} \tag{12.10}$$

$$\rho = (X^2 + Y^2)^{1/2} \tag{12.11}$$

$$r' = (X'^2 + Y'^2)^{1/2}$$

$\theta$ = angle between $\vec{X}'$ and the projection of $\vec{X}$ in the X'Y' plane.

r' and $\theta$ are like the usual polar coordinates corresponding to the rectangular coordinates X' and Y' except that instead of $\theta$ being measured from the X' axis, it is changed by a constant (in the prime coordinates) so that it is measured from the projection of $\vec{X}$ in the X'Y' plane. Therefore dX'dY' is replaced with r'dr'd$\theta$ when making a change in variables in Eq. (12.5). Note

$$(X - X')^2 + (Y - Y')^2 + (Z)^2 = |\vec{X} - \vec{X}'|^2 = (\vec{X} - \vec{X}')\cdot(\vec{X} - \vec{X}')$$

$$= r^2 + r'^2 - 2\,\vec{X}\cdot\vec{X}' = r^2 + r'^2 - 2\,(X\hat{e}_1 + Y\hat{e}_2)\cdot\vec{X}'$$

$$= r^2 + r'^2 - 2\rho r'\cos\theta.$$

Eq. (12.5) becomes

$$\psi(\vec{X}) = \frac{V_a Z}{2\pi} \int_o^{2\pi} \int_o^{M} [r^2 + r'^2 - 2\rho r'\cos\theta]^{-3/2} \, r'dr'd\theta.$$

The integration in r' can be performed using direct methods and the result is

$$\psi(\vec{X}) = \frac{V_a Z}{2\pi} \int_o^{2\pi} \left\{ \frac{M\rho\cos\theta - r^2}{(r^2 - p^2\cos^2\theta)\,(M^2 - 2\rho M\cos\theta + r^2)^{1/2}} + \frac{r}{(r^2 - \rho^2\cos^2\theta)} \right\} d\theta \,. \qquad (12.12)$$

Eq. (12.12) is one solution to Laplace's equation. Another solution is obtained by defining $\phi$ by

$$\phi(X,Y,Z) = - \text{Im}\, \psi(iX,iY,iZ) \,. \qquad (12.13)$$

If the square roots in Eqs. (12.10) and (12.11) are regarded as the principal determinations, multiplying the coordinates by i means replacing $\rho$ and r with $i\rho$ and ir. Eq. (12.13) becomes

$$\phi(X,Y,Z) = -\text{Im}\left[ \frac{V_a iZ}{2\pi} \int_o^{2\pi} \left\{ \frac{iM\rho\cos\theta + r^2}{(\rho^2\cos^2\theta - r^2)\,(M^2 - 2i\rho M\cos\theta - r^2)^{1/2}} - \frac{ir}{r^2 - \rho^2\cos^2\theta} \right\} d\theta \right]$$

or

$$\phi(X,Y,Z) = \text{Re}\left[ \frac{V_a Z}{\pi} \int_o^{\pi} \frac{iM\rho\cos\theta + r^2}{\left(r^2 - \rho^2\cos^2\theta\right)\left(M^2 - 2i\rho M\cos\theta - r^2\right)^{1/2}} \, d\theta \right] . \qquad (12.14)$$

What has been obtained so far is another solution to Laplace's equation, given by Eq. (12.14), where once again all coordinates are regarded as real. It remains to be seen if this is the solution we are looking for. It suffices to show that Eq. (12.14) reduces to Eq. (2.1) when X = Y = 0, i.e., when $\rho = 0$ and r = Z. Making the substitutions and evaluating the integral yields

$$\phi(0,0,Z) = \frac{V_a Z}{[M^2 - Z^2]^{1/2}}$$

which is the same as Eq. (2.1) if

$$V_a = \frac{V_o}{L} \, [M^2 - L^2]^{1/2}$$

and Eq. (2.5) has been verified.

As an incidental point, if we were looking for a solution to the boundary value problem that is valid for $r > M$, we would seek a solution to Laplace's equation that joins smoothly (continuous potential and electric field) with Eq. (12.14). Requiring a smooth connection is how the specification of the potential on the Z axis (Eq. 2.1)) "propagates" from the region with $r < M$ to the region with $r > M$. The reader is left to his own resources to find this solution.

## SECTION 13

## PRELIMINARY DISCUSSION ON THE APPLICATION OF THE LEAST ACTION PRINCIPLE

### A. INTRODUCTION

Let $\phi_{actual}$ represent the potential at an arbitrary point in space between the electrode and grounded plane. Let $\phi$ denote some other function that is arbitrary except for two restrictions. The first restriction is that $\phi$ be smooth (twice differentiable with respect to the coordinates X,Y,Z). The second restriction is that $\phi$ satisfy the boundary conditions imposed on the potential. Therefore, $\phi$ is to be zero on the XY plane, zero at infinity, and equal to $V_o$ on the electrode surface. It is well known (see, for example, Chapter 19 of Ref. 20) that any $\phi$ satisfying the above conditions will also satisfy

$$\int |\vec{\nabla}\phi_{actual}|^2 d^3X \leq \int |\vec{\nabla}\phi|^2 d^3X \ . \tag{13.1}$$

The volume integrals are over all space outside of the electrode and to the right of the grounded plane. The left side of Eq. (13.1) can be recognized as the energy stored in the field (to within proportionality constants). $\phi$ might be thought of as an imagined or fictitious potential and the right side of Eq. (13.1) would be regarded as the energy (to within proportionality constants) stored in the fictitious field. For example, $\phi$ might be a function that is intended to serve as an approximation for the actual potential. $-\vec{\nabla}\phi$ would then provide the approximation for the electric field and the right side of Eq. (13.1) is the approximation for the energy stored in the field. This approximation of the energy stored in the field will, according to Eq. (13.1), always be greater than (or equal to if $\phi = \phi_{actual}$) the correct energy stored in the field. It should be emphasized that, in order to qualify for this discussion, $\phi$ must satisfy the same boundary conditions that the actual potential satisfies.

Since $\phi$ will be referred to much more frequently than the actual potential, the word "potential" will refer to $\phi$ and "electric field" will refer to the negative gradient of $\phi$. If reference to the actual potential or actual electric field are intended, the phrases "actual potential" or "actual electric field" will be used. Similarly, "energy" refers to the right side of Eq. (13.1). If reference to the left side is intended, the phrase "actual energy" will be used. To avoid the need of frequently writing $\varepsilon_o/2$, "energy" or "actual energy" is used loosely and refers to the terms in Eq. (13.1). The only exception is at the end of Section 14 where capacitance in MKS units is calculated from energy and the correct proportionality constants are used.

The objective of the sections to follow is to obtain an estimate of the energy stored in the field. From this, capacitance can be calculated. The basic strategy is to use some kind of scheme to construct a function $\phi$ that is intended to be a rough approximation of the actual potential. The energy

calculated from the right side of Eq. (13.1) will serve as an approximation for the actual energy stored in the field. Most of the analysis to follow is dedicated to finding schemes for constructing $\phi$. Since any estimate of the energy (that is not exactly correct) will be too large, the most accurate estimate is the smallest estimate, and this makes it possible to compare different estimates to see which estimate (and which $\phi$) is the best without knowing what the actual potential is.

The remainder of this section will discuss some general properties that $\phi$ will be constructed to have. These properties alone will not uniquely determine $\phi$. There will still be some "adjustability" left in $\phi$, i.e., some characteristics will be left unspecified. The remaining sections consider different ways of specifying the remaining characteristics.

## B. THE EQUIPOTENTIAL SURFACES

One way to specify a function is to specify two independent properties: the geometric shape of the equipotential surfaces (the function is being called a potential here) and the value of the potential associated with each equipotential surface. The shapes of the equipotential surfaces are taken to be geometrically similar to the electrode surface. They differ from the electrode surface only by a translation, which can be described in terms of where the left side of the surface intersects the Z axis, and a scale factor. The way the scale factor varies with the intercept will be left unspecified in this section. It probably seems that no matter how the scale factor varies with the intercept, this is a crude representation of the actual equipotential surfaces, especially since at large distances the actual equipotential surfaces resemble those from a dipole. The equipotential surfaces produced by $\phi$ will probably not have a close resemblance at large distances to those of a dipole. But at large distances, large enough that the actual field resembles a dipole, there is not much energy stored in the field. If this is also true for the field produced by $\phi$, accuracy at large distances will not be needed to estimate the stored energy. Of course even at close distances, the agreement between the equipotential surfaces of $\phi$ and the actual equipotential surfaces may be (depending on the electrode shape) crude no matter how the scale factor of the surface is made to vary with the intercept. Fortunately, it often happens that even crude approximations of the field lead to accurate estimates of the stored energy or capacitance. The big advantage in stipulating the geometry of the equipotential surfaces to be as stated is that the problem is mathematically manageable.

Let the surface that is obtained by translating the electrode, so that its left intercept (the word "intercept" will refer to the Z coordinate of the intersection of a given surface with the Z axis. "Left" or "right" refers to Fig. 5.1) is at the origin, be given by the equation

$$G(X,Y,Z) = 0 \ . \tag{13.2}$$

This implies that a solution to

$$G(0,0,Z) = 0 \tag{13.3}$$

is

$$Z = 0 \ . \tag{13.4}$$

The equation of the electrode at its original location is obtained by translating Eq. (13.2) a distance L in the +Z direction so that the left intercept is at Z = L. The equation is

$$\text{Equation of electrode surface: } G(X,Y,Z - L) = 0. \tag{13.5}$$

A surface that is similar to the electrode surface, differing only by the intercept and a scale factor, has the equation

$$G(KX,KY,KZ) = 0 \ .$$

The surface given by the above equation has its left intercept at Z = 0 because Eq. (13.4) is a solution to Eq. (13.3) and therefore Z = 0 is a solution to G(0,0,KZ) = 0. A surface with a scale factor given by K and left intercept at some $Z = Z_0$ is obtained by translating the above equation in Z to the point $Z_0$. The result is

Surface with scale factor 1/K and intercept $Z_0$:

$$G(KX,KY,K(Z - Z_0)) = 0 \ . \tag{13.6}$$

K is the inverse scale factor. As K increases, the surface gets smaller. As $K \to 0$, the surface becomes infinitely large.

The fictitious potential will be constructed so that each equipotential surface can be expressed by Eq. (13.6) for some K and $Z_0$. Different equipotential surfaces will have different scale factors and different intercepts. If K is changed, the equipotential surface is changed and therefore $Z_0$ is changed, i.e., there is a one-to-one correspondence between K and $Z_0$. Therefore, to specify the family of equipotential surfaces, we can either specify K as a function of $Z_0$ or we can specify $Z_0$ as a function of K. The first convention will be used and we write

Equipotential surface with left intercept at $Z_0$:

$$G(K(Z_0)X,\ K(Z_0)Y,\ K(Z_0)(Z - Z_0)) = 0. \tag{13.7}$$

The function G is determine by the electrode surface. Once the function K has been specified, the family of equipotential surfaces will be completely determined.

## C. INTERPRETING $Z_o$ AS A FUNCTION OF COORDINATES

K is to be regarded as a fixed function of $Z_o$, although it has not yet been decided which function it is, so the family of equipotential surfaces, given by Eq. (13.7), has been defined. For any given point in space, there will be one equipotential surface that this point lies on. The surface has a left intercept at some $Z_o$. This allows us to geometrically define $Z_o$ as a function of the coordinates. At any given (X,Y,Z), we define $Z_o(X,Y,Z)$ to be the left intercept of the equipotential surface that passes through (X,Y,Z). An analytical statement of this definition is provided by Eq. (13.7). For any given (X,Y,Z), Eq. (13.7) can be used, in principle at least, *to solve for $Z_o$ and this defines it as a function of the* coordinates. Eq. (13.7) can be used for either of two purposes. If $Z_o$ is specified, Eq. (13.7) can be used to find the set of points that lie on the surface having left intercept $Z_o$. Or, if a point is specified, Eq. (13.7) can be used to solve for $Z_o$.

$\phi$ and $Z_o$ can both be expressed as a function of the coordinates (X,Y,Z) and there is a connection between them. Each can be expressed as a function of the other. $\phi(X,Y,Z)$ is the potential of the equipotential surface that passes through X,Y,Z while $Z_o(X,Y,Z)$ is the left intercept of that very same surface. Since there is an invertible mapping between the potential of a surface and the intercept of a surface, there is an invertible mapping between $\phi$ and $Z_o$. This implies that there exists a function F satisfying

$$\phi(X,Y,Z) = F(Z_o(X,Y,Z)) \ . \tag{13.8}$$

The function F can easily be related to $\phi$. Since (X,Y,Z) and $(0,0,Z_o(X,Y,Z))$ are two points that lie on the same equipotential surface, the potentials at those two points are equal and we have

$$\phi(X,Y,Z) = F(Z_o(X,Y,Z)) = \phi(0,0,Z_o(X,Y,Z)) = V(Z_o(X,Y,Z)) \ . \tag{13.9}$$

The function that $\phi$ is of $Z_o$ is the function that $\phi$ is of its third argument when the first two arguments are zero, i.e., F is V.

## D. ELECTRIC FIELD

After K has been specified, the family of equipotential surfaces, given by Eq. (13.7), is completely determined. But this does not yet specify the function $\phi(X,Y,Z)$ because an association between the equipotential surfaces and the values of the potential on the surfaces has not yet been specified. One way to specify this is to specify the electric field strength, E(Z) on the Z axis. Once functions have been chosen for E and K, the potential $\phi$ is completely determined.

The electric field vector at an arbitrary point in space can be expressed in terms of E times a quantity that depends only on the geometry of the equipotential surfaces by a simple application of the chain rule. As was stated above, $Z_o$ can be regarded as a function of the coordinates and the potential can be expressed as a function of the single variable $Z_o$. The chain rule gives

$$\vec{\varepsilon} = -\vec{\nabla}\phi = -\frac{d\phi}{dZ_o}\vec{\nabla}Z_o .$$

But from Eq. (13.9) we have

$$\frac{d\phi}{dZ_o} = \frac{dV}{dZ_o}(Z_o) .$$

The expression on the right of the above equation is the magnitude of the electric field strength on the Z axis evaluated at $Z = Z_o$. Therefore

$$\frac{d\phi}{dZ_o} = E(Z_o) \tag{13.10}$$

and we get

$$\vec{\varepsilon} = -E(Z_o)\,\vec{\nabla}Z_o . \tag{13.11}$$

## E. CONSTRAINTS

The potential is specified when the functions $E(Z_o)$ and $K(Z_o)$ have been specified. These functions are not completely arbitrary because some constraints must be satisfied. An obvious constraint on E required to satisfy the boundary condition is

$$\int_0^L E(Z_o)dZ_o = V_o . \tag{13.12}$$

One constraint on K is obtained by noting that the equipotential surface is required to approach the electrode surface as the intercept approaches L. Therefore

$$K(Z_o) \to 1 \quad \text{as} \quad Z_o \to L . \tag{13.13}$$

Also, as the intercept of the equipotential surface gets closer to the grounded plane, the size of the surface increases without bound which implies

$$K(Z_o) \to 0 \quad \text{as} \quad Z_o \to 0 . \tag{13.14}$$

Another constraint comes from the requirement that equipotential surfaces don't intersect. One surface must be completely contained inside another. From this point on, it will be assumed that the surfaces are everywhere convex. Then a necessary and sufficient condition for one surface, $S_2$, to enclose another surface, $S_1$, without intersection is that the left intercept of $S_2$ be less than the left intercept of $S_1$ and the right intercept of $S_2$ be greater than the right intercept of $S_1$. Stated another way, if we move from one equipotential surface to another in such a way that the left intercept is decreasing, it is required that the right intercept be increasing, i.e., the right intercept must be a strictly decreasing function of the left intercept. Consider a surface with left intercept $Z_o$ and scale factor $1/K(Z_o)$. Let D be the distance between the intercepts of the electrode.

The distance between intercepts for the given surface must be $D/K(Z_o)$. The right intercept for the given surface is at

$$\text{Right Intercept} = Z_o + \frac{D}{K(Z_o)} \quad . \tag{13.15}$$

The requirement is that this expression be a decreasing function of $Z_o$, i.e., the derivative with respect to $Z_o$ is negative. This gives

$$\frac{DK'}{K^2} > 1 \quad . \tag{13.16}$$

But it is also required that Eq. (13.14) be satisfied. This can be assured if Eq. (13.16) is replaced with a stronger statement. A requirement that is stronger than the requirement that the derivative of Eq. (13.15) be negative is to require not only that the derivative be negative but that it also becomes negatively infinite as $Z_o \to 0$. Physically, this is saying that if the left intercept is very close to the grounded plane, a tiny decrease in the left intercept produces a large increase in the right intercept. The right intercept goes to infinity as the left intercept goes to zero. This statement is equivalent to Eq. (13.14). The stronger condition that will replace Eq. (13.16) is

$$\frac{DK'}{K^2} > 1 \text{ for all } Z_o \text{ and becomes positively infinite as } Z_o \to 0 \quad . \tag{13.17}$$

## F. ENERGY STORED IN THE FIELD IN TERMS OF E AND K

To within proportionality constants, the energy stored in the field is

$$\text{Energy} = \int |\vec{\nabla}\phi|^2 d^3X = \int |\vec{\varepsilon}|^2 d^3X \tag{13.18}$$

where the volume integral is over all space outside of the electrode and to the right of the grounded plane. From Eq. (13.11) this becomes

$$\text{Energy} = \int E^2(Z_o) |\vec{\nabla} Z_o|^2 d^3X \quad . \tag{13.19}$$

Let $\theta_1$ and $\theta_2$ be two surface coordinates on a constant $Z_o$ surface and let the coordinates be chosen so that $\theta_1$, $\theta_2$, $Z_o$ forms an orthogonal system of generalized coordinates. Let $h_1$, $h_2$, and $h_3$ be the scale factors associated with the coordinates $\theta_1$, $\theta_2$, $Z_o$ (the scale factors associated with the coordinates, which are explained on page 24 of Ref. 18, are not to be confused with the scale factor 1/K which is associated with the surface). The volume integral can be expressed as

$$\text{Energy} = \int E^2(Z_o) |\vec{\nabla} Z_o|^2 \, h_1 h_2 h_3 d\theta_1 d\theta_2 dZ_o .$$

But $h_3$ is given by (see page 24 of Ref. 18)

$$h_3 = \left[\left(\frac{\partial Z_o}{\partial X}\right)^2 + \left(\frac{\partial Z_o}{\partial Y}\right)^2 + \left(\frac{\partial Z_o}{\partial Z}\right)^2\right]^{-1/2} = \frac{1}{|\vec{\nabla} Z_o|}$$

so that

$$\text{Energy} = \int E^2(Z_o)|\vec{\nabla} Z_o|\ h_1 h_2 d\theta_1 d\theta_2 dZ_o.$$

The double integral

$$\int E^2(Z_o)|\vec{\nabla} Z_o| h_1 h_2 d\theta_1 d\theta_2$$

is a surface integral on a $Z_o$ = constant surface. Since $E^2(Z_o)$ is constant on that surface, it factors out of the double integral and the result is

$$\text{Energy} = {}_0\int^L E^2(Z_o)\left\{\int |\vec{\nabla} Z_o| dS\right\} dZ_o. \tag{13.20}$$

The inside integral represents a surface integral on a $Z_o$ = constant surface.

The next step is to find another expression for the gradient of $Z_o$. $Z_o$ is defined as a function of the coordinates through Eq. (13.7) and its gradient can be calculated by implicit differentiation. It will be convenient to have different symbols that represent different interpretations of the partial derivative. Due to a scarcity of good symbols, the symbol that usually represents total derivative will be used as one of them. Letting $X_i$ represent any of the coordinates X, Y, or Z, the symbol $d/dX_i$ will denote partial derivative with respect to the $X_i$ coordinate with $Z_o$ treated as a function of the coordinates. $\partial/\partial X_i$ will denote partial derivative with respect to the $X_i$ coordinate with $Z_o$ treated as constant. Subscripts to G represent derivatives with respect to the indicated arguments. Eq. (13.7) is satisfied identically in the coordinates when it defines $Z_o$ as a function of the coordinates (i.e., when $Z_o$ is treated as a variable) so

$$\frac{dG}{dX_i}(K(Z_o)X, K(Z_o)Y, K(Z_o)(Z - Z_o)) = 0. \tag{13.21}$$

On the other hand, if $Z_o$ is treated as constant, Eq. (13.7) is satisfied only when the coordinates lie on the appropriate surface. In this case the gradient of G is a vector that is perpendicular to the surface. To make a unit vector out of the gradient, we divide by the magnitude to get

$$\frac{\sum_i \frac{\partial G}{\partial X_i}(K(Z_o)X, K(Z_o)Y, K(Z_o)(Z - Z_o))\,\hat{e}_i}{\left[\sum_i \left(\frac{\partial G}{\partial X_i}\right)^2\right]^{1/2}} = \hat{S} \tag{13.22}$$

where $\hat{S}$ is a unit vector perpendicular to the surface. The chain rule applied to Eq. (13.22) yields

$$\frac{\sum_i G_i \hat{e}_i}{\left[\sum_i (G_i)^2\right]^{1/2}} = \hat{S} \tag{13.23}$$

and applied to Eq. (13.21) yields

$$G_1\left(XK'\frac{dZ_o}{dX_i} + K\frac{dX}{dX_i}\right) + G_2\left(YK'\frac{dZ_o}{dX_i} + K\frac{dY}{dX_i}\right)$$

$$+ G_3\left((Z - Z_o)K'\frac{dZ_o}{dX_i} + K\frac{dZ}{dX_i} - K\frac{dZ_o}{dX_i}\right) = 0$$

where $K' = dK/dZ_o$. $dX/dX_i$ is 1 if $X_i = X$ and zero otherwise, etc., for $dY/dX_i$ and $dZ/dX_i$. Rearranging gives

$$[K'(G_1X + G_2Y + G_3(Z - Z_o)) - KG_3]\frac{dZ_o}{dX_i} + KG_i = 0 \ .$$

Dividing by the magnitude of the gradient of G and using Eq. (13.23) yields

$$\frac{dZ_o}{dX_i} = \frac{-KS_i}{K'\left[S_1X + S_2Y + S_3\left(Z - Z_o - \frac{K}{K'}\right)\right]} \ .$$

If $\hat{n}$ denotes the outer normal to the surface, $\hat{S}$ is plus or minus $\hat{n}$. But a change in the sign of S does not effect the above expression so S can be replaced with the outer normal n. The equation finally becomes

$$\vec{\nabla}Z_o = \frac{-K\hat{n}}{K'\left[n_1X + n_2Y + n_3\left(Z - Z_o - \frac{K}{K'}\right)\right]} \ . \tag{13.24}$$

From Eq. (13.24) it is seen that $\vec{\nabla}Z_o$ is either parallel or antiparallel to the outer normal of the surface. We can predict that $\vec{\nabla}Z_o$ is antiparallel to the outer normal by looking at an arbitrary point and noting the surface that passes through that point. If the point moves perpendicular to the surface in

the direction of the outer normal, it will move to a larger surface having a smaller left intercept. So $Z_o$ decreases when the point of evaluation moves in the direction of the outer normal which implies that the component of the gradient of $Z_o$ in the direction of the outer normal is negative. Note that K' is positive since K is increasing so the above conclusion together with Eq. (13.24) implies

$$n_1X + n_2Y + n_3\left(Z - Z_o - \frac{K}{K'}\right) > 0 \quad . \tag{13.25}$$

As a check for consistency, note that the expression in Eq. (13.25) is the scalar product between the outer normal and the position vector with origin at $(0,0,Z_o + K/K')$. This origin is clearly to the right of the left intercept. Also, the right intercept is at $Z_o + D/K$ and from Eq. (13.16) we have it that the origin is to the left of the right intercept. So Eq. (13.16) ensures that the position vector, whose scalar product with the outer normal is represented by Eq. (13.25), is measured from a point that is inside the surface. Since the surface is assumed to be convex, the scalar product is positive. Incidentally, the implication also goes the other way. If Eq. (13.25) is satisfied for all (X,Y,Z) on the surface, it is also satisfied when $X = Y = 0$, $Z = Z_o + D/K$, $n_1 = n_2 = 0$, $n_3 = 1$. This produces Eq. (13.16). So, if the surface is convex, Eq. (13.16) is satisfied if and only if Eq. (13.25) is satisfied everywhere on the surface. The two conditions are equivalent.

Since $-\vec{\nabla}Z_o$ is parallel to the outer normal,

$$|\vec{\nabla}Z_o|dS = -\vec{\nabla}Z_o \cdot d\vec{S}$$

where $d\vec{S}$ is in the direction of the outer normal. Putting this and Eq. (13.24) into Eq. (13.20) yields

$$\text{Energy} = \int_0^L E^2(Z_o)\left\{\int \frac{K\hat{n} \cdot d\vec{S}}{K'\left[n_1X + n_2Y + n_3\left(Z - Z_o - \frac{K}{K'}\right)\right]}\right\}dZ_o. \tag{13.26}$$

Since all equipotential surfaces are geometrically similar, the surface integral in Eq. (13.26) can be related to a surface integral on the electrode surface. Since the coordinates X,Y,Z lie on the surface given by Eq. (13.7), the new coordinates

$$X' = KX, \; Y' = KY, \; Z' = K(Z - Z_o) + L$$

lie on the surface given by

$$G(X',Y',Z' - L) = 0$$

which is Eq. (13.5), the equation of the electrode surface. An element of surface area in the prime coordinates is related to that in the unprimed coordinates by

$$dS' = K^2dS \quad .$$

The point X,Y,Z and the original surface taken together have a similar geometry as the point X',Y',Z' and the electrode surface taken together. So the normal to the original surface evaluated at X,Y,Z equals the normal to the electrode surface evaluated at X',Y',Z'. In other words,

$$\hat{n}(X,Y,Z) = \hat{n}'(X',Y',Z') .$$

Making the substitutions results in

$$\int \frac{\hat{n} \cdot d\vec{S}}{n_1 X + n_2 Y + n_3\left(Z - Z_o - \frac{K}{K'}\right)} = \frac{1}{K^2} \int \frac{\hat{n}' \cdot d\vec{S}'}{\frac{n_1 X'}{K} + \frac{n_2 Y'}{K} + n_3\left(\frac{Z' - L}{K} - \frac{K}{K'}\right)} .$$

We can drop the primes by explicitly showing what surfaces the integrations are on. $S_L$ will denote the electrode surface and $S(Z_o)$ will denote the surface with intercept at $Z_o$. We get

$$\int_{S(Z_o)} \frac{\hat{n} \cdot d\vec{S}}{n_1 X + n_2 Y + n_3\left(Z - Z_o - \frac{K}{K'}\right)}$$

$$= \frac{1}{K} \int_{S_L} \frac{\hat{n} \cdot d\vec{S}}{n_1 X + n_2 Y + n_3\left(Z - L - \frac{K^2}{K'}\right)} . \qquad (13.27)$$

Eq. (13.26) becomes

$$\text{Energy} = \int_0^L \frac{E^2(Z_o)}{K'(Z_o)} \left\{ \int_{S_L} \frac{\hat{n} \cdot d\vec{S}}{n_1 X + n_2 Y + n_3\left(Z - L - \frac{K^2}{K'}\right)} \right\} dZ_o . \qquad (13.28)$$

To obtain an estimate of the energy, the functions represented by $E(Z_o)$ and $K(Z_o)$ must be selected so that the integral in the above equation can be evaluated. This is the subject of the remaining sections.

## SECTION 14

## DERIVATION OF EQUATION 3.2

An upper bound on the energy stored in the field can be obtained by selecting some E and K compatible with the constraints and using Eq. (13.28). There are several tempting choices. For example, if $K^2/K'$ were constant, the surface integral in Eq. (13.28) would not depend on $Z_o$ and could be factored out as a constant and the calculations would be simplified. Unfortunately, this choice of K does not satisfy Eq. (13.17) or Eq. (13.14). It is also tempting to use Eq. (10.10), the model field, for E. But if this is done, the choice of possible Ks becomes more restricted because there is a strong tendency for the integral to produce singularities. Another approach is to make a completely ad hoc selection. This author has tried several and the choice of functions that produced Eq. (3.2) seems to be the best of the few that were tested.

The K used here is given by

$$K(Z_o) = \frac{DZ_o}{L^2 + LD - Z_o^2} \quad . \tag{14.1}$$

A simple calculation will show that

$$\frac{K'}{K^2} = \frac{Z_o^2 + L^2 + DL}{DZ_o^2} \quad . \tag{14.2}$$

It is evident that the constraints given by Eq. (13.13) and Eq. (13.17) are satisfied. The electric field on the Z axis is given by

$$E(Z_o) = \frac{A}{L^2 + LD - Z_o^2} \tag{14.3}$$

where A is a constant that must be adjusted to satisfy the constraint given by Eq. (13.12). Using this to evaluate A produces

$$A = \frac{2V_o(L^2 + LD)^{1/2}}{\ln\left(\frac{(L^2 + LD)^{1/2} + L}{(L^2 + LD)^{1/2} - L}\right)} \quad . \tag{14.4}$$

Interchanging the order of integration in Eq. (13.28) and substituting for E and K yields

$$\text{Energy} = \frac{A^2}{D} \int \int \frac{dZ_o dS}{Z_o^2 \hat{n} \cdot \vec{r}_R + (DL + L^2) \hat{n} \cdot \vec{r}_L} \tag{14.5}$$

where

$$\vec{r}_R = X\hat{e}_1 + Y\hat{e}_2 + (Z - L - D)\hat{e}_3$$
$$\vec{r}_L = X\hat{e}_1 + Y\hat{e}_2 + (Z - L)\hat{e}_3 \tag{14.6}$$

$\vec{r}_R$ and $\vec{r}_L$ are the position vectors measured from the right and left intercepts of the electrode. The $Z_o$ integration can be performed directly and the result is

$$\text{Energy} = \frac{A^2 B}{D} \int \frac{1}{[(\vec{r}_L \cdot \hat{n})(\vec{r}_R \cdot \hat{n})]^{1/2}} \text{Tan}^{-1}\left(\text{LB}\left[\frac{\vec{r}_R \cdot \hat{n}}{\vec{r}_L \cdot \hat{n}}\right]^{1/2}\right) dS$$

where

$$B = [L^2 + LD]^{-1/2} . \tag{14.7}$$

Since the integration is done on a surface of revolution, the integral can be expressed as a line integral on the curve defined by the intersection of the electrode with the positive X half of the XZ plane. Simply replace dS with $2\pi X d\ell$. Also, it is now time to use the correct proportionality constants. If $\varepsilon_o$ represents the permittivity constant, the energy in the MKS system of units is given by

$$\text{Energy} = \frac{A^2 B \varepsilon_o \pi}{D} \int \frac{X}{[(\vec{r}_L \cdot \hat{n})(\vec{r}_R \cdot \hat{n})]^{1/2}} \text{Tan}^{-1}\left(\text{LB}\left[\frac{\vec{r}_R \cdot \hat{n}}{\vec{r}_L \cdot \hat{n}}\right]^{1/2}\right) d\ell \quad . \tag{14.8}$$

Eqs. (14.8), (14.7), (14.4), and (3.1) produce Eq. (3.2).

Several times in the analysis that produced Eq. (3.28), it was assumed that the surface is everywhere convex. If this condition is satisfied and if the curve defined by the intersection of the electrode in the XZ plane is everywhere convex, the integrand in Eq. (14.8) will remain finite. To see this, note that the only possibilities for a singularity occur when $\vec{r}_R \cdot \hat{n} \to 0$ or $\vec{r}_L \cdot \hat{n} \to 0$. If $\vec{r}_R \cdot \hat{n} \to 0$, the argument to the inverse tangent goes to zero and the inverse tangent approaches the value of its argument and the term that

goes to zero divides out. The only remaining possibility for a singularity occurs when $\vec{r}_L \cdot \hat{n} \to 0$. To show that this also does not produce a singularity, it suffices to show that

$$\frac{X}{(\vec{r}_L \cdot \hat{n})^{1/2}}$$

remains finite, or that

$$\frac{X^2}{\vec{r}_L \cdot \hat{n}}$$

remains finite. Note that $\hat{n}$ is an outer normal so

$$\hat{n} = \frac{dZ}{d\ell}\,\hat{e}_1 - \frac{dX}{d\ell}\,\hat{e}_3$$

and

$$\vec{r}_L \cdot \hat{n} = X\,\frac{dZ}{d\ell} - (Z - L)\,\frac{dX}{d\ell}$$

so

$$\frac{X^2}{\vec{r}_L \cdot \hat{n}} = \frac{1}{\frac{1}{X}\frac{dZ}{dX} - \frac{Z - L}{X^2}} \tag{14.9}$$

where we have used

$$\frac{d}{d\ell} = \frac{dX}{d\ell}\,\frac{d}{dX}$$

which approaches d/dX when the point of evaluation approaches the left intercept (the only possible location for a singularity). It suffices to show that the denominator in Eq. (14.9) does not go to zero. To evaluate the limit of the denominator, use l'Hospital's Rule to get

$$\lim_{X \to 0} \left( \frac{1}{X}\frac{dZ}{dX} - \frac{Z - L}{X^2} \right) = \frac{1}{2}\,\frac{d^2Z}{dX^2}$$

which is not zero if the curve is convex.

SECTION 15

# INCREASING THE ACCURACY OF THE CAPACITANCE ESTIMATE

The best capacitance or energy estimate comes from the field that produces the smallest energy that the constraints will allow. The constraints are (1) the requirement that the equipotential surfaces be given by Eq. (13.7), and (2) that E and K satisfy Eqs. (13.12), (13.13), and (13.17). Making the energy as small as possible (by adjusting E and K) will produce the best approximation for the field in some sense of "best approximation." It is obviously the best approximation in the sense of producing the best estimate of the stored energy. It is also the best approximation in another well-known sense which will be briefly reviewed. Note

$$\int |\vec{\varepsilon} - \vec{\varepsilon}_{actual}|^2 d^3X = \int \varepsilon^2 d^3X + \int \vec{\varepsilon}_{actual} \cdot (\vec{\varepsilon}_{actual} - 2\vec{\varepsilon})\, d^3X$$

$$= \int \varepsilon^2 d^3X + \int \vec{\nabla}\phi_{actual} \cdot \vec{\nabla}(\phi_{actual} - 2\phi)\, d^3X \quad .$$

Using Green's first identity,

$$\int \vec{\nabla}\phi_{actual} \cdot \vec{\nabla}(\phi_{actual} - 2\phi)\, d^3X = \int (\phi_{actual} - 2\phi)\, \vec{\nabla}\phi_{actual} \cdot d\vec{S}$$

$$- \int (\phi_{actual} - 2\phi)\, \nabla^2\phi_{actual}\, d^3X \quad .$$

The volume integral on the far right is obviously zero. The surface integral is over all boundary surfaces but since the potentials are zero on all boundaries except the electrode, the surface integral can be taken to be on the electrode surface where $\phi_{actual} - 2\phi = V_o - 2V_o = -V_o$. $d\vec{S}$ is at present an inner normal (to the electrode) but the sense can be changed by multiplying by -1 and the result is

$$\int \vec{\nabla}\phi_{actual} \cdot \vec{\nabla}(\phi_{actual} - 2\phi)\, d^3X = V_o \int \vec{\nabla}\phi_{actual} \cdot d\vec{S}$$

$$= -V_o \int \vec{\varepsilon}_{actual} \cdot d\vec{S}$$

so that

$$\int |\vec{\varepsilon} - \vec{\varepsilon}_{actual}|^2 d^3X = \int \varepsilon^2 d^3X - V_o \int \vec{\varepsilon}_{actual} \cdot d\vec{S} \quad . \tag{15.1}$$

As an incidental point, the surface integral in Eq. (15.1) is proportional to the charge on the electrode. If we let $\varepsilon$ be zero, the equation relates the energy stored in the actual field to the charge on the electrode. This, together with the definition of capacitance, provides a derivation of the relationship between capacitance and energy. This derivation doesn't require that we recognize the equivalence between energy stored in the field and energy required to charge the capacitor.

The left side of Eq. (15.1) is the continuum version of the square error in the electric field. Therefore, minimizing the energy, which minimizes the right side (and therefore the left side) of Eq. (15.1), produces the best approximation in the sense of least square error in the electric field. There is another way to look at this. Note that the fictitious electric field already has a zero curl, since it was derived from a potential, and the boundary conditions on the potential are built into the problem. The only thing left to specify in order to completely determine $\vec{\varepsilon}$ is its divergence. The actual field has zero divergence so the best approximation is obtained by making $\vec{\varepsilon}$ have as "close to a zero divergence" as the constraints will allow. We can think of the process of minimizing the energy as a process of finding the field that has a "best fit" to zero divergence. From the equivalence between minimizing the energy and obtaining the least square error in the electric field, it is evident that the interpretation of "best fit" to zero divergence is least square error with a field (the actual field) that really has a zero divergence.

The above discussion applies to the general case of adjusting a field to minimize the energy. But when the electric field has the kind of structure that we have been working with (i.e., the adjustability is through the functions E and K), there is yet another, but equivalent, interpretation that can be given to "best fit" to zero divergence. To find this interpretation, we will use the Euler equation (sometimes called the Euler-Lagrange equations, these equations are discussed in Refs. 18 and 21, or any advanced classical mechanics textbook) to minimize the energy which is given by Eq. (13.28). The need to include the constraint Eq. (13.12) as a subsidiary condition can be avoided if we work with $V(Z_o)$ instead of $E(Z_o)$ where $E(Z_o) = dV(Z_o)/dZ_o$. Instead of working with a constraint, we are now working with a fixed end-point problem in the variable V. We will first minimize Eq. (13.28) in V with K regarded as an arbitrary but fixed function. Euler's equation gives

$$\left\{\frac{\partial}{\partial V} - \frac{d}{dZ_o}\frac{\partial}{\partial V'}\right\}\left\{\frac{(V')^2}{K'}\int_L \frac{\hat{n}\cdot\vec{dS}}{n_1X + n_2Y + n_3\left(Z - L - \frac{K^2}{K'}\right)}\right\} = 0 \quad .$$

The expression that is being operated on does not explicitly contain V so the differential equation has the first integral (with E replacing V')

$$\frac{E(Z_o)}{K'(Z_o)}\int_L \frac{\hat{n}\cdot\vec{dS}}{n_1X + n_2Y + n_3\left(Z - L - \frac{K^2(Z_o)}{K'(Z_o)}\right)} = A \qquad (15.2)$$

where A is a constant. Eq. (15.2) can be made to look familiar by reversing some of the steps made in Section 13. By using Eqs. (13.27) and (13.24), Eq. (15.2) becomes

$$-E(Z_o) \int_{S(Z_o)} \vec{\nabla} Z_o \cdot d\vec{S} = A \quad .$$

$E(Z_o)$ can be moved inside the integral since the integration is on a constant $Z_o$ surface and Eq. (13.11) gives

$$\int_{S(Z_o)} \vec{\varepsilon} \cdot d\vec{S} = A = \text{constant} \quad . \tag{15.3}$$

Eq. (15.3) states that the optimum E for any given K is the function that will make the electric field have the same surface integral on all equipotential surfaces. This result could have been anticipated because we know that we are seeking a field that has the "best fit" to a zero divergence and we could have guessed that constant surface integrals on the equipotential surfaces is a good candidate for defining this best fit. However, the requirement of constant surface integrals is not complete because this condition can be satisfied for any admissible function K and different choices of K will produce different field patterns.

The constant A can be evaluated from the requirement of Eq. (13.12) and the result is

$$A = \frac{V_o}{\int_0^L \left\{ \int_{S_L} \frac{\hat{n} \cdot d\vec{S}}{K'\left[n_1 X + n_2 Y + n_3\left(Z - L - \frac{K^2}{K'}\right)\right]} \right\}^{-1} dZ_o} \quad . \tag{15.4}$$

Using Eq. (15.2), Eq. (13.28) can be expressed as

$$\text{Energy} = \int_0^L E(Z_o)\, A\, dZ_o = A \int_0^L E(Z_o) dZ_o = AV_o \quad .$$

Using Eq. (15.4) gives

$$\text{Energy} = \frac{V_o^2}{\int_0^L K' \left\{ \int_{S_L} \frac{dS}{n_1 X + n_2 Y + n_3\left(Z - L - \frac{K^2}{K'}\right)} \right\}^{-1} dZ_o} \quad . \tag{15.5}$$

All that remains is to select a function K. Once this has been done, the integral in Eq. (15.5) can be evaluated numerically. It will probably be helpful to convert the surface integral into a line integral as was done in Section 14. An adjustment in the energy will be needed to include the proportionality constants appropriate for the system of units that will be used.

One possible choice for K is given by Eq. (14.1). This was the choice used to get Eq.(3.2). Since Eq. (15.5) automatically includes the optimum $E(Z_o)$ for any choice of $K(Z_o)$, and Eq. (3.2) used a randomly selected $E(Z_o)$, using the same K in both equations will result in Eq. (15.5) having the greater accuracy. If the reader can find a K that will produce a smaller estimate, the accuracy will be even higher.

This would be a good place to end this discussion except that the reader must be wondering why there has not been any attempt to find the optimum K. The reason is mathematical complexity. If the reader would like to pursue this analysis, the following steps may help him to get started.

The objective is to find the K that will minimize the right side of Eq. (15.5), so we want to maximize the integral. Let F be the integrand so that

$$F = K' \left\{ \int_{S_L} \frac{dS}{n_1 X + n_2 Y + n_3 \left( Z - L - \frac{K^2}{K'} \right)} \right\}^{-1} . \qquad (15.6)$$

The only $Z_o$ dependence in this expression is implicit through the K and K' so Euler's equation has a first integral (see page 19 of Ref. 21) which is

$$F - K' \frac{\partial F}{\partial K'} = C = \text{constant} .$$

A brute force calculation of the derivative $\partial F/\partial K'$ substituted into the above equation will produce

$$K^2 \int_{S_L} \frac{n_3 dS}{\left[ n_1 X + n_2 Y + n_3 \left( Z - L - \frac{K^2}{K'} \right) \right]^2} = C \left[ \int_{S_L} \frac{dS}{n_1 X + n_2 Y + n_3 \left( Z - L - \frac{K^2}{K'} \right)} \right]^2 .$$

The above equation is supposed to be solved for K or, at least, some expression that can be substituted into Eq. (15.5) is to be solved. At this stage the mathematical complexity is enough to overwhelm this author and the reader is on his own if he wishes to continue.

## REFERENCES


1. Garrett, H. B., "The Charging of Spacecraft Surfaces," Reviews of Geophysics and Space Physics, Vol. 19, No. 4, November 1981.

2. Shaw, R. R., J. E. Nanevicz, and R. C. Adamo, "Observations of Electrical Discharges Caused by Differential Satellite-Charging," Published as Paper SA41, Spacecraft Charging by Magnetospheric Plasmas, Progress in Astronautics and Aeronautics, Vol. 47, for the American Geophysical Union Spring Annual Meeting, Washington, DC, June 1975, MIT Press, 1976.

3. Morse, Philip M., and Herman Feshbach, "Methods of Theoretical Physics," Part II, McGraw-Hill Book Company, 1953.

4. Ramo, Simon, John R. Whinnery, and Theodore Van Duzer, "Fields and Waves in Communication Electronics," John Wiley and Sons, Inc., 1965.

5. Farrall, G. A., "Electrical Breakdown in Vacuum," IEEE Transactions on Electrical Insulation, Vol. EI-20, No. 5, October 1985.

6. Garrett, H. B., and C. P. Pike, editors, "Space Systems and Their Interactions with Earth's Space Environment," Progress in Astronautics and Aeronautics, Vol. 71, Martin Summerfield, Series Editor-in-Chief, New York University, 1980.

7. Leung, P., and G. Plamp, "Characteristics of RF Resulting From Dielectric Discharges," IEEE Transactions on Nuclear Science, Vol. NS 29, pp. 1610-1614, 1982.

8. Grier, N. T., "Plasma Interaction Experiment II Laboratory and Flight Results," USAF/NASA Spacecraft Environmental Interactions Technology Conference, Abstracts, 4-6 October 1983.

9. Miller, W. L., "An Investigation of Arc Discharging on Negatively-Biased Dielectric-Conductor Samples in a Plasma," USAF/NASA Spacecraft Environmental Interactions Technology Conference, Abstracts, 4-6 October 1983.

10. McMahon, Eugene J., "A Tutorial on Treeing," IEEE Transactions on Electrical Insulation, Vol. EI-13, No. 4, August 1978.

11. Cuddihy, E. F., "A Concept for the Intrinsic Dielectric Strength of Electrical Insulation Materials," JPL Publication 85-30, April 15, 1985.

12. Hlawiczka, Paul, "Introduction to Quantum Electronics," Academic Press, 1971.

13. Cookson, Alan H., "Gas-Insulated Cables," IEEE Transactions on Electrical Insulation, Vol. EI-20, No. 5, October 1985.

14. Forster, E. O., "The Search for Universal Features of Electrical Breakdown in Solids, Liquids and Gases," IEEE Transactions on Electrical Insulation, Vol. EI-17, No. 6, December 1982.

15. Berger, S., "Onset or Breakdown Voltage Reduction by Electrode Surface Roughness in Air and $SF_6$," IEEE, Vol. PAS-95, No. 4, July/August 1976.

16. Jackson, John David, "Classical Electrodynamics," Second Edition, John Wiley and Sons, Inc., 1975.

17. Arfken, G., "Mathematical Methods for Physicists," Second Edition, Academic Press, 1970.

18. Morse, Philip M., and Herman Feshbach, "Methods of Theoretical Physics," Part I, McGraw-Hill Book Company, 1953.

19. Greenleaf, Frederick P., "Introduction to Complex Variables," W. B. Saunders Company, 1972.

20. Feynman, Richard P., Robert B. Leighton, and Matthew Sands, "The Feynman Lectures on Physics," Volume II, Addison-Wesley Publishing Company, Sixth Printing, February 1977.

21. Gelfand, I. M., and S. V. Fomin, "Calculus of Variations," Prentice-Hall, Inc., 1963.

# APPENDIX

Some example electrode shapes are shown on the following pages. Each page contains several curves, each curve defining the shape of a different electrode, and a data table. For each electrode shown, the data table lists several quantities as follows:

R/L: Radius of curvature of apex of electrode divided by distance from grounded plane to apex of electrode.

(V/E)/L: V/E is the ratio of the potential of the electrode to the electric field at the apex of the electrode. (V/E)/L is this ratio divided by distance from grounded plane to apex of electrode. The entries in the "ACTUAL" column are values that are accurate to the number of digits displayed. The entries in the "CALCULATED" column are the approximations that are obtained from Eq. (1.1). The "% ERROR" column shows the error that results from using Eq. (1.1). A positive (or negative) error indicates that the calculated value is too high (or low). Note that (V/E)/L is dimensionless.

CAP/L: Capacitance of the grounded plane-electrode system divided by the distance from grounded plane to electrode. The entries in the "ACTUAL" column are values that are accurate to the number of digits displayed. The entries in the "CALCULATED" column are the approximations that are obtained from Eq. (3.2). The "%ERROR" column shows the error that results from using Eq. (3.2). The error is always positive because Eq. (3.2) always produces an overestimate. "NA" will appear in the "CALCULATED" and "% ERROR" columns when an electrode does not have the required convex shape, and Eq. (3.2) contains undefined quantities. It can occasionally happen that Eq. (3.2) can be used on a shape that is not everywhere convex. There are numerical entries in the "CALCULATED" and "% ERROR" columns whenever the calculation could be made.

An attempt to find an example shape that matches an actual electrode can be made the following way. First, glance through the examples and note the ones that have a shape that reasonably resembles the actual electrode. Out of this set of examples (if there are any), select the one having an R/L that approximates the R/L for the actual electrode. Judgment will be needed when making a compromise between accuracy in shape and accuracy in R/L. The choice is likely to depend on whether it is V/E or capacitance that is of interest.

Assuming that one of the example electrodes accurately fits the actual electrode in both shape and in R/L (which is not likely, but is possible), estimates of V/E and capacitance can be obtained the following way. Find the entry in the "ACTUAL" column under (V/E)/L for the example electrode. Multiply this entry by the distance from grounded plane to apex of the actual electrode. The result will be V/E for the actual electrode in the same units in which the distance was expressed. Now find the entry in the "ACTUAL" column under (CAP/L) for the example electrode. Multiply this entry by the distance from grounded

plane to apex of the actual electrode. The result will be the capacitance of the actual electrode. If the distance was expressed in meters, the capacitance will be in farads.

The above procedure can be used if one of the example electrodes happens to accurately represent the actual electrode. If not, the primary usefulness of the examples is to give some feeling for the kind of error that should be expected when using Eq. (1.1) or Eq. (3.2). This information is found in the "% ERROR" columns.

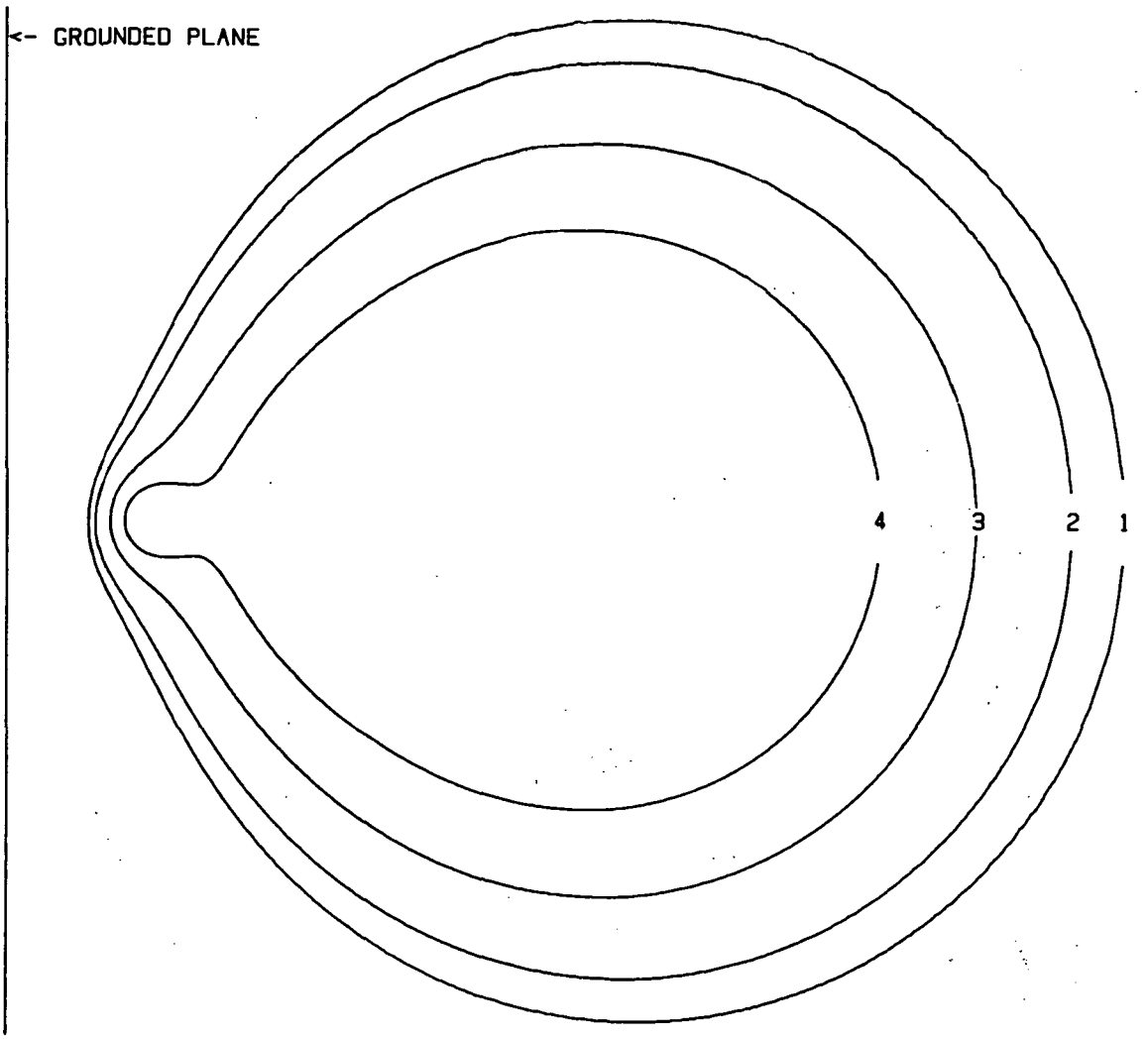


| CURVE # | R/L | (V/E)/L ACTUAL | (V/E)/L CALCULATED | (V/E)/L %ERROR | CAP/L (FARADS/METER) ACTUAL | CAP/L (FARADS/METER) CALCULATED | CAP/L (FARADS/METER) %ERROR |
|---|---|---|---|---|---|---|---|
| 1 | 1.44E 00 | 6.98E-01 | 6.83E-01 | -2.1 | 1.24E-09 | 1.93E-09 | 56.0 |
| 2 | 1.07E 00 | 6.34E-01 | 6.16E-01 | -2.8 | 9.94E-10 | NA | NA |
| 3 | 5.79E-01 | 4.83E-01 | 4.65E-01 | -3.7 | 6.47E-10 | NA | NA |
| 4 | 2.91E-01 | 3.09E-01 | 3.04E-01 | -1.7 | 4.03E-10 | NA | NA |

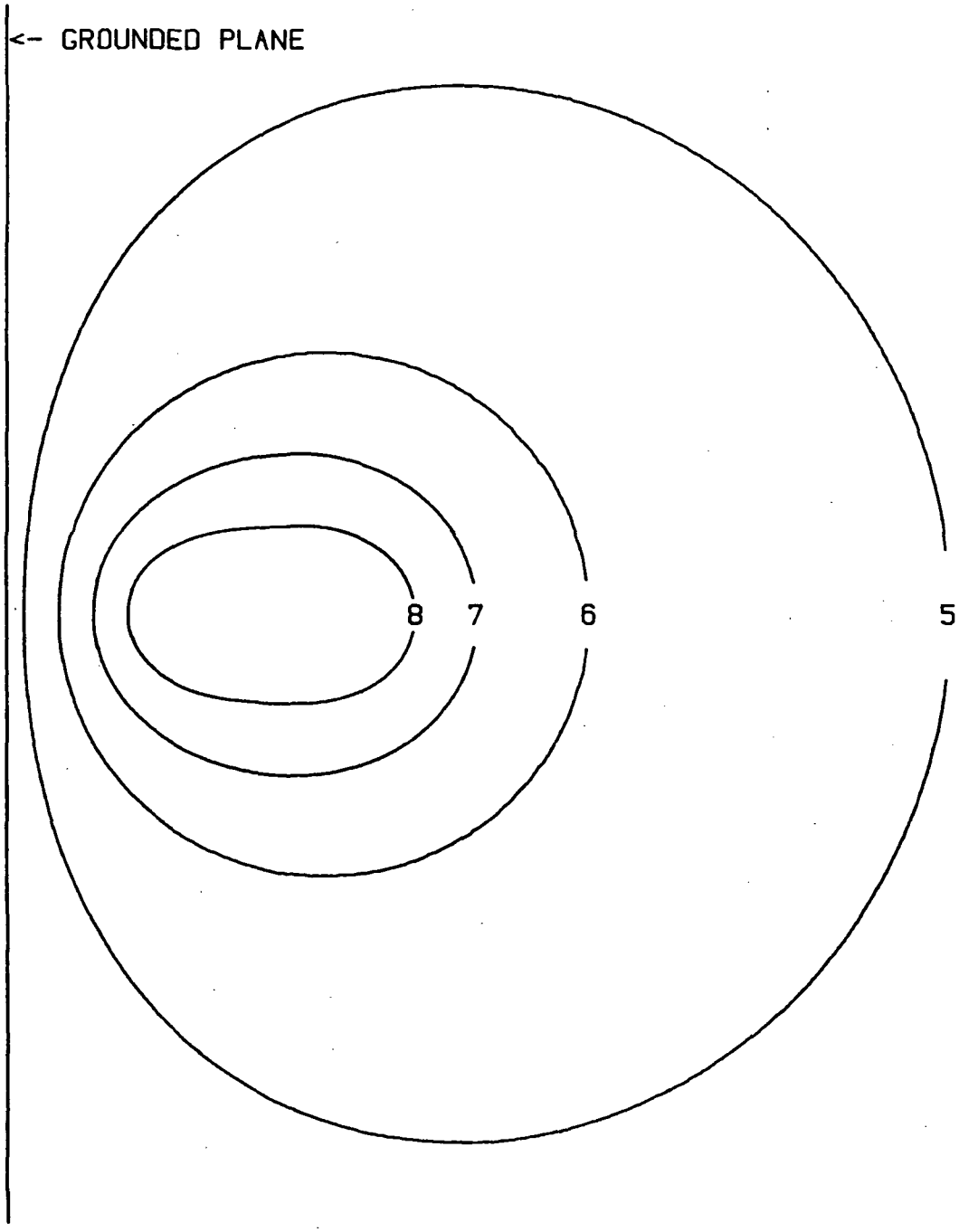


| CURVE # | R/L | (V/E)/L ACTUAL | (V/E)/L CALCULATED | %ERROR | CAP/L (FARADS/METER) ACTUAL | CAP/L (FARADS/METER) CALCULATED | %ERROR |
|---|---|---|---|---|---|---|---|
| 5 | 4.65E 01 | 9.86E-01 | 9.86E-01 | 0.0 | 9.97E-09 | 1.20E-08 | 20.6 |
| 6 | 4.88E 00 | 8.77E-01 | 8.80E-01 | 0.3 | 1.04E-09 | 1.29E-09 | 24.1 |
| 7 | 1.52E 00 | 6.80E-01 | 6.95E-01 | 2.1 | 3.27E-10 | 4.20E-10 | 28.4 |
| 8 | 5.48E-01 | 4.24E-01 | 4.51E-01 | 6.4 | 1.27E-10 | 1.74E-10 | 36.5 |

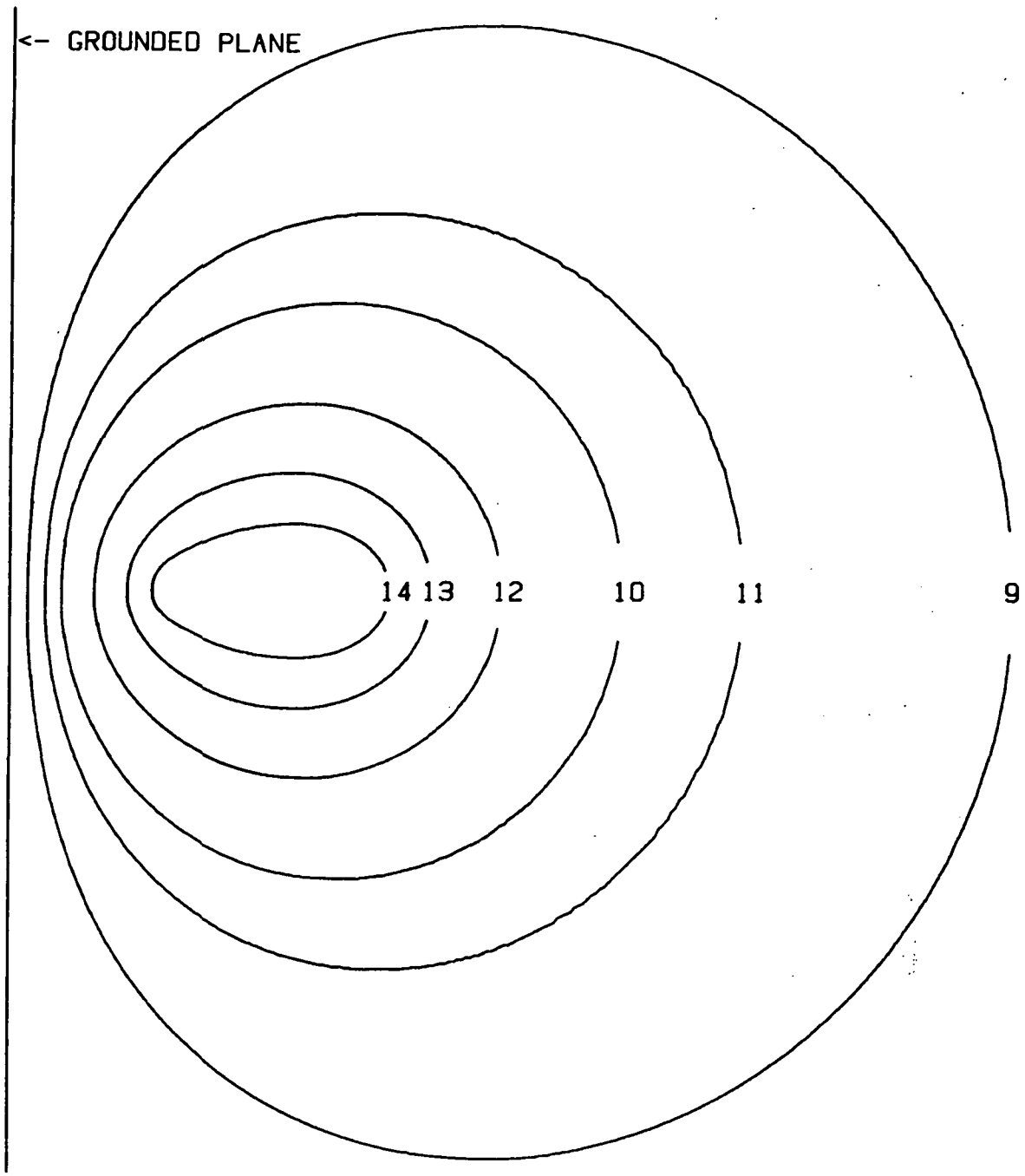


| CURVE # | R/L | (V/E)/L ACTUAL | (V/E)/L CALCULATED | (V/E)/L %ERROR | CAP/L (FARADS/METER) ACTUAL | CAP/L (FARADS/METER) CALCULATED | CAP/L (FARADS/METER) %ERROR |
|---|---|---|---|---|---|---|---|
| 9 | 5.53E 01 | 9.88E-01 | 9.88E-01 | 0.0 | 1.17E-08 | 1.42E-08 | 20.9 |
| 10 | 5.80E 00 | 8.95E-01 | 8.97E-01 | 0.2 | 1.24E-09 | 1.55E-09 | 25.1 |
| 11 | 1.35E 01 | 9.53E-01 | 9.53E-01 | 0.0 | 2.88E-09 | 3.54E-09 | 23.2 |
| 12 | 1.79E 00 | 7.21E-01 | 7.29E-01 | 1.1 | 3.98E-10 | 5.10E-10 | 28.0 |
| 13 | 6.37E-01 | 4.77E-01 | 4.88E-01 | 2.3 | 1.63E-10 | 2.19E-10 | 34.4 |
| 14 | 2.21E-01 | 2.44E-01 | 2.49E-01 | 1.8 | 7.77E-11 | 1.18E-10 | 51.4 |

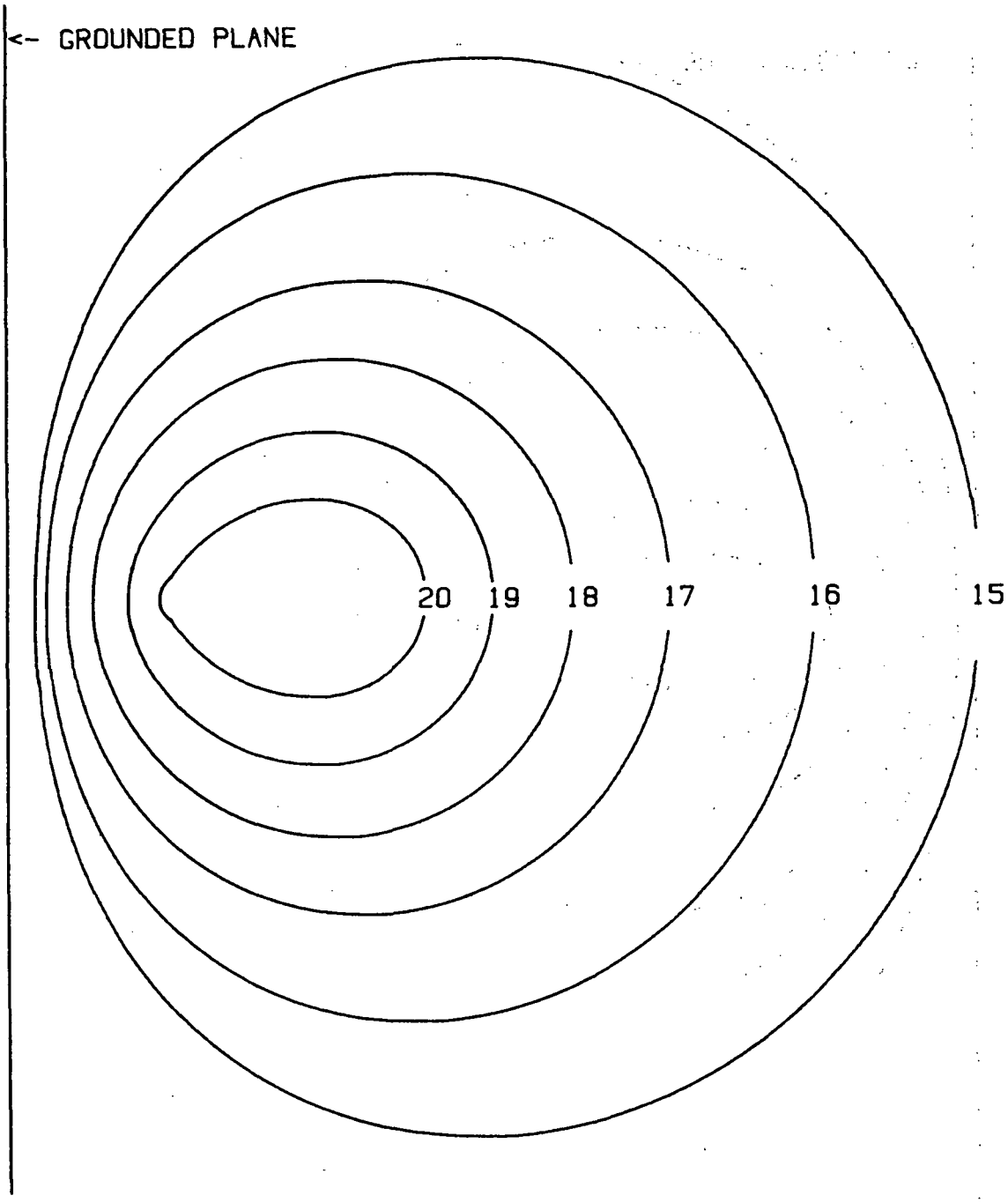


| CURVE # | R/L | (V/E)/L ACTUAL | (V/E)/L CALCULATED | (V/E)/L %ERROR | CAP/L (FARADS/METER) ACTUAL | CAP/L (FARADS/METER) CALCULATED | CAP/L (FARADS/METER) %ERROR |
|---|---|---|---|---|---|---|---|
| 15 | 3.21E 01 | 9.80E-01 | 9.80E-01 | 0.0 | 6.42E-09 | 7.84E-09 | 22.1 |
| 16 | 1.41E 01 | 9.54E-01 | 9.55E-01 | 0.0 | 2.82E-09 | 3.47E-09 | 23.2 |
| 17 | 5.56E 00 | 8.91E-01 | 8.93E-01 | 0.2 | 1.12E-09 | 1.41E-09 | 25.2 |
| 18 | 2.47E 00 | 7.83E-01 | 7.88E-01 | 0.5 | 5.15E-10 | 6.61E-10 | 28.2 |
| 19 | 9.26E-01 | 5.83E-01 | 5.81E-01 | -0.3 | 2.26E-10 | 3.01E-10 | 33.3 |
| 20 | 1.68E-01 | 2.50E-01 | 2.01E-01 | -19.4 | 9.67E-11 | 1.46E-10 | 51.4 |

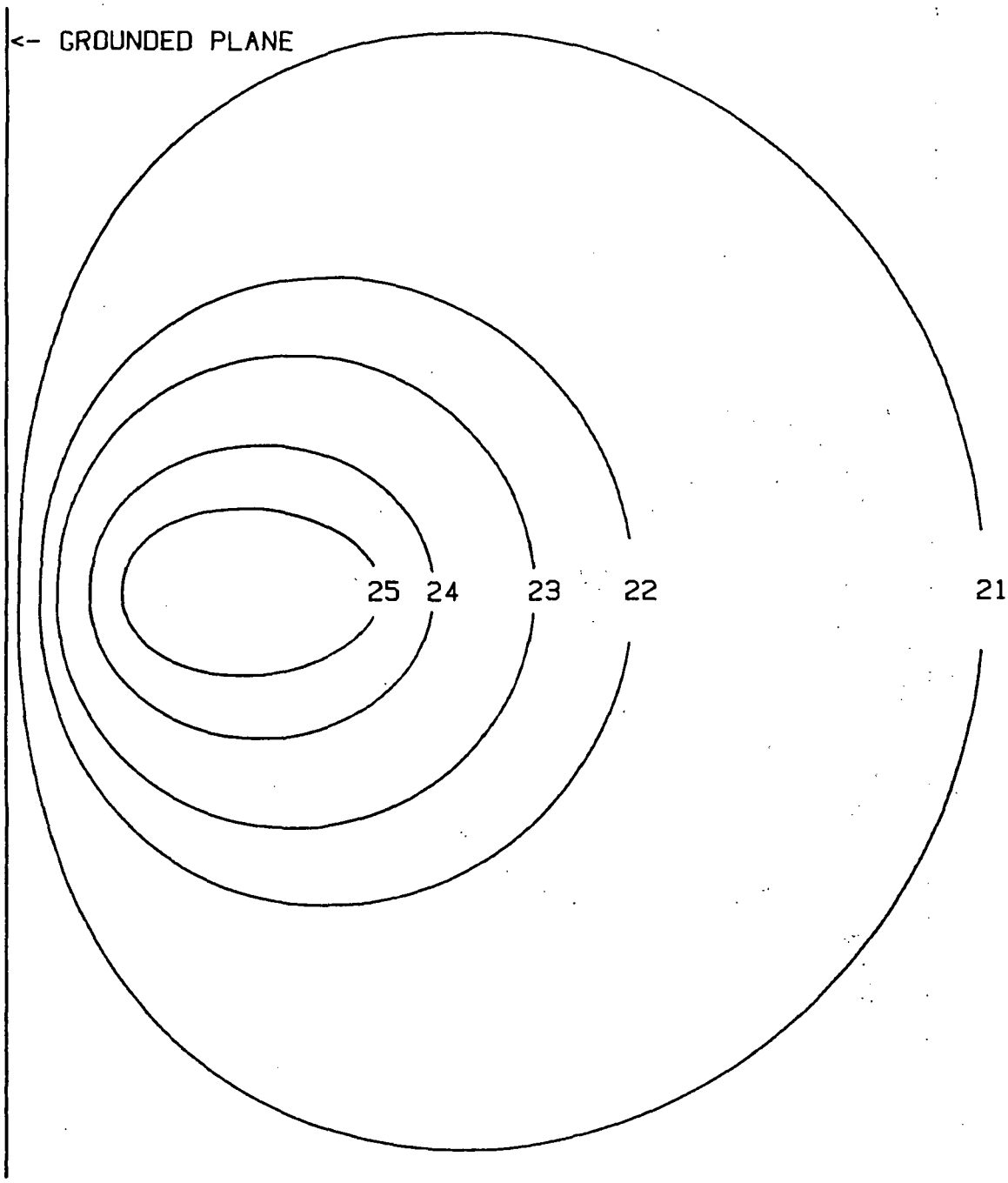


| CURVE # | R/L | (V/E)/L ACTUAL | (V/E)/L CALCULATED | (V/E)/L %ERROR | CAP/L (FARADS/METER) ACTUAL | CAP/L (FARADS/METER) CALCULATED | CAP/L (FARADS/METER) %ERROR |
|---|---|---|---|---|---|---|---|
| 21 | 8.18E 01 | 9.92E-01 | 9.92E-01 | 0.0 | 1.66E-08 | 2.02E-08 | 21.3 |
| 22 | 1.13E 01 | 9.43E-01 | 9.44E-01 | 0.1 | 2.28E-09 | 2.80E-09 | 22.7 |
| 23 | 4.84E 00 | 8.76E-01 | 8.79E-01 | 0.4 | 9.74E-10 | 1.22E-09 | 24.8 |
| 24 | 1.51E 00 | 6.78E-01 | 6.94E-01 | 2.3 | 3.06E-10 | 3.96E-10 | 29.6 |
| 25 | 5.49E-01 | 4.24E-01 | 4.52E-01 | 6.6 | 1.19E-10 | 1.62E-10 | 36.2 |

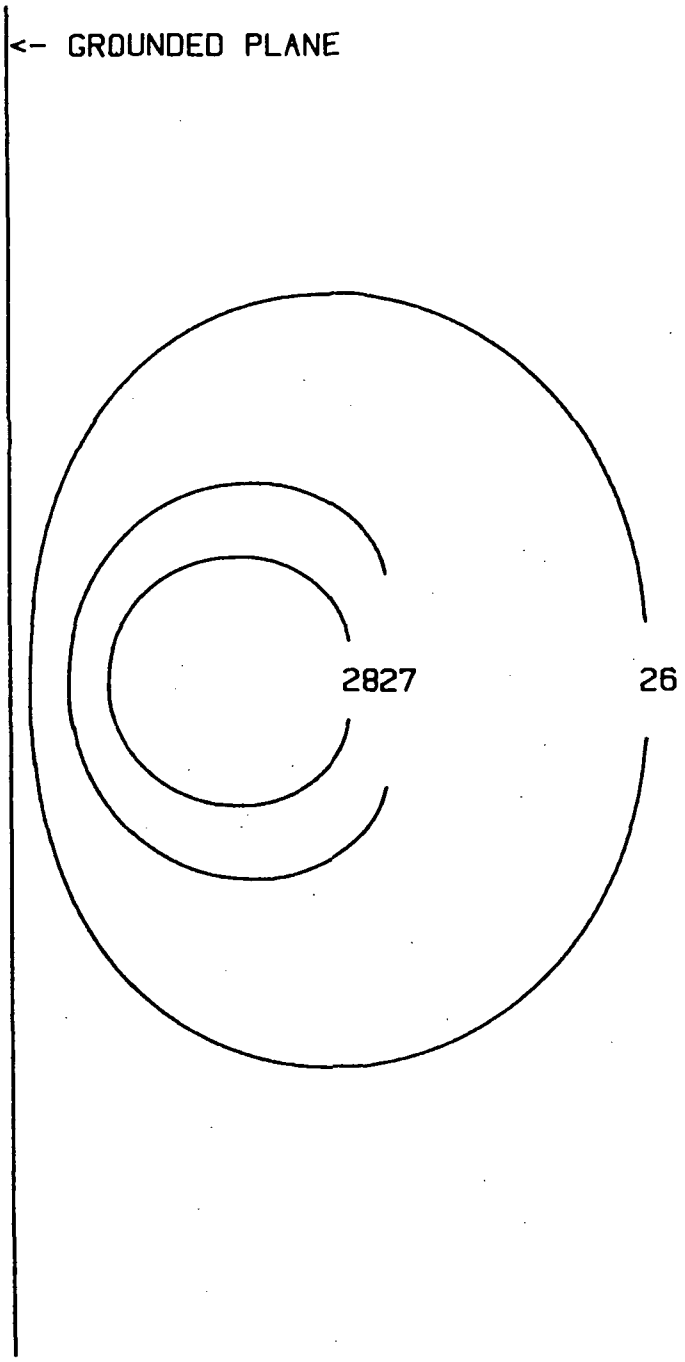


| CURVE # | R/L | (V/E)/L ACTUAL | (V/E)/L CALCULATED | %ERROR | CAP/L (FARADS/METER) ACTUAL | CAP/L (FARADS/METER) CALCULATED | %ERROR |
|---|---|---|---|---|---|---|---|
| 26 | 3.76E 01 | 9.82E-01 | 9.83E-01 | 0.0 | 6.16E-09 | 7.82E-09 | 27.0 |
| 27 | 4.02E 00 | 8.52E-01 | 8.58E-01 | 0.7 | 6.35E-10 | 8.40E-10 | 32.2 |
| 28 | 1.29E 00 | 6.33E-01 | 6.60E-01 | 4.2 | 1.93E-10 | 2.83E-10 | 46.2 |

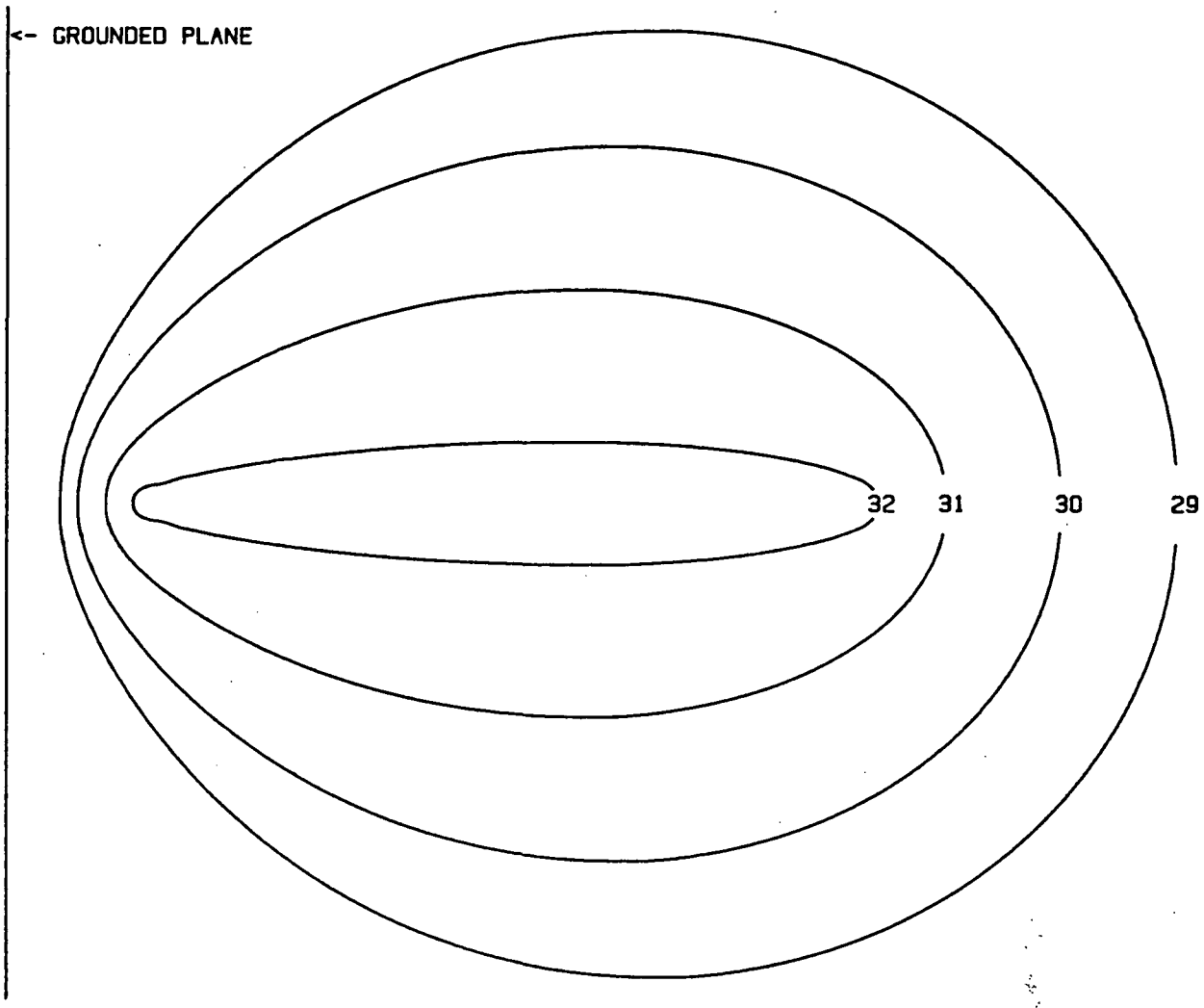


| CURVE # | R/L | (V/E)/L ACTUAL | (V/E)/L CALCULATED | (V/E)/L %ERROR | CAP/L (FARADS/METER) ACTUAL | CAP/L (FARADS/METER) CALCULATED | CAP/L (FARADS/METER) %ERROR |
|---|---|---|---|---|---|---|---|
| 29 | 4.13E 00 | 8.61E-01 | 8.61E-01 | -0.0 | 1.98E-09 | 2.43E-09 | 22.4 |
| 30 | 2.01E 00 | 7.52E-01 | 7.51E-01 | -0.2 | 1.04E-09 | 1.32E-09 | 26.7 |
| 31 | 6.61E-01 | 5.06E-01 | 4.98E-01 | -1.5 | 4.39E-10 | 6.18E-10 | 40.9 |
| 32 | 1.26E-01 | 1.60E-01 | 1.59E-01 | -0.4 | 1.54E-10 | 3.34E-10 | 117.4 |

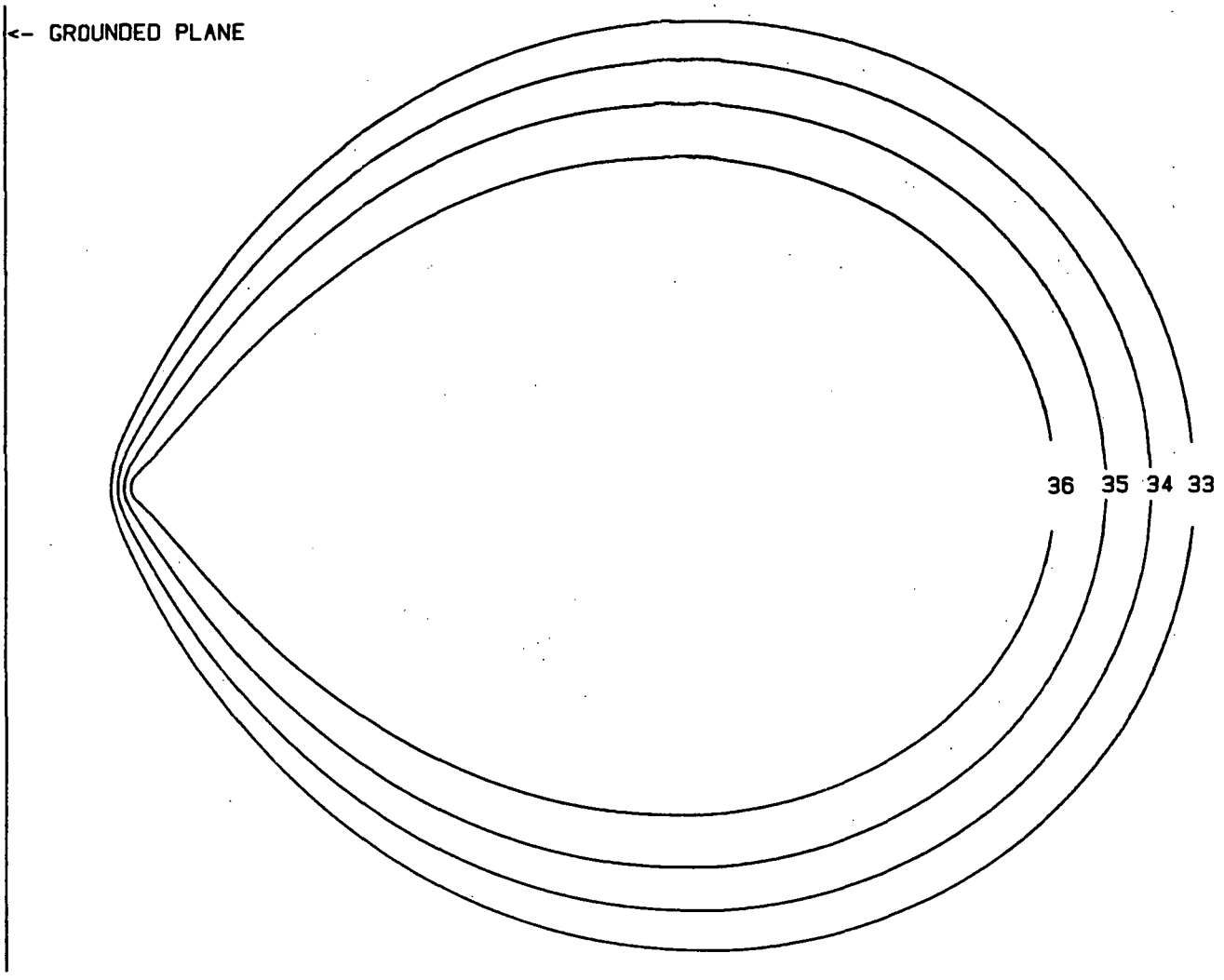


| CURVE # | R/L | (V/E)/L ACTUAL | (V/E)/L CALCULATED | (V/E)/L %ERROR | CAP/L (FARADS/METER) ACTUAL | CAP/L (FARADS/METER) CALCULATED | CAP/L (FARADS/METER) %ERROR |
|---|---|---|---|---|---|---|---|
| 33 | 7.43E-01 | 5.93E-01 | 5.27E-01 | -11.2 | 8.61E-10 | 1.21E-09 | 40.7 |
| 34 | 4.87E-01 | 5.05E-01 | 4.22E-01 | -16.3 | 7.18E-10 | 1.07E-09 | 48.8 |
| 35 | 2.92E-01 | 3.94E-01 | 3.04E-01 | -22.7 | 5.90E-10 | 9.69E-10 | 64.1 |
| 36 | 1.51E-01 | 2.58E-01 | 1.85E-01 | -28.3 | 4.67E-10 | 1.00E-09 | 114.1 |

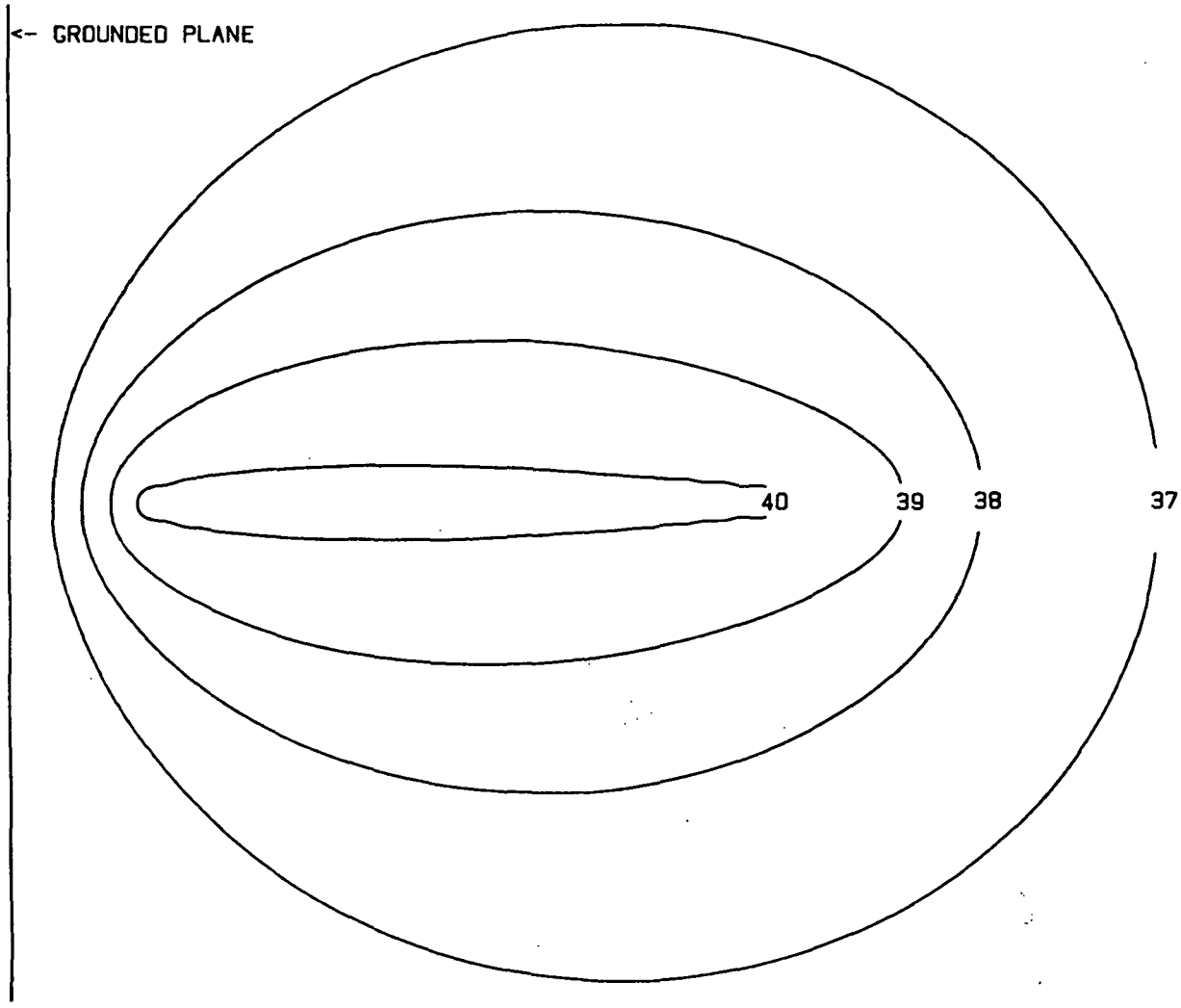


| CURVE # | R/L | (V/E)/L ACTUAL | (V/E)/L CALCULATED | (V/E)/L %ERROR | CAP/L (FARADS/METER) ACTUAL | CAP/L (FARADS/METER) CALCULATED | CAP/L (FARADS/METER) %ERROR |
|---|---|---|---|---|---|---|---|
| 37 | 6.41E 00 | 9.05E-01 | 9.06E-01 | 0.0 | 2.65E-09 | 3.16E-09 | 19.5 |
| 38 | 1.90E 00 | 7.39E-01 | 7.40E-01 | 0.1 | 8.60E-10 | 1.08E-09 | 25.3 |
| 39 | 6.36E-01 | 4.89E-01 | 4.88E-01 | -0.2 | 3.57E-10 | 4.90E-10 | 37.4 |
| 40 | 1.25E-01 | 1.54E-01 | 1.58E-01 | 2.6 | 1.21E-10 | NA | NA |